applied sciences

MDPI

Review

Biochar for Wastewater Treatment—Conversion Technologies and Applications

Ghizlane Enaime [1], Abdelaziz Baçaoui [1], Abdelrani Yaacoubi [1] and Manfred Lübken [2,*]

[1] Laboratory of Applied Chemistry, Unity of Methodology and Environment, Faculty of Sciences Semlalia, Cadi Ayyad University, Marrakech B.P. 2390, Morocco; ghizlane.ennaime@ced.uca.ma (G.E.); bacaoui@uca.ac.ma (A.B.); ayaacoubi@uca.ac.ma (A.Y.)

[2] Institute of Urban Water Management and Environmental Engineering, Ruhr-Universität Bochum, Universitätsstraße 150, 44801 Bochum, Germany

* Correspondence: manfred.luebken@rub.de

Received: 16 April 2020; Accepted: 13 May 2020; Published: 18 May 2020

Abstract: Biochar as a stable carbon-rich material shows incredible potential to handle water/wastewater contaminants. Its application is gaining increasing interest due to the availability of feedstock, the simplicity of the preparation methods, and their enhanced physico-chemical properties. The efficacy of biochar to remove organic and inorganic pollutants depends on its surface area, pore size distribution, surface functional groups, and the size of the molecules to be removed, while the physical architecture and surface properties of biochar depend on the nature of feedstock and the preparation method/conditions. For instance, pyrolysis at high temperatures generally produces hydrophobic biochars with higher surface area and micropore volume, allowing it to be more suitable for organic contaminants sorption, whereas biochars produced at low temperatures own smaller pore size, lower surface area, and higher oxygen-containing functional groups and are more suitable to remove inorganic contaminants. In the field of water/wastewater treatment, biochar can have extensive application prospects. Biochar have been widely used as an additive/support media during anaerobic digestion and as filter media for the removal of suspended matter, heavy metals and pathogens. Biochar was also tested for its efficiency as a support-based catalyst for the degradation of dyes and recalcitrant contaminants. The current review discusses on the different methods for biochar production and provides an overview of current applications of biochar in wastewater treatment.

Keywords: biochar; thermal conversion; modification; adsorption; wastewater treatment

1. Introduction

The world's water resources are being deteriorated due to the continuous discharge of a large number of organic and inorganic contaminants such as dyes, heavy metals, surfactants, pharmaceuticals, pesticides, and personal care products from industries and municipalities into water bodies [1]. Most of these pollutants are highly persistent in nature and are otherwise convert into recalcitrant form [2]. The uncontrolled discharge of these pollutants is a concern because of their suspected negative effects on ecosystems [1,3,4]. Several conventional technologies are applied worldwide for the removal of wastewater pollutants including coagulation-flocculation, adsorption, membrane filtration, reverse osmosis, chemical precipitation, ion-exchange, electrochemical treatment, solvent extraction and flotation for the removal of inorganic pollutants [5–8]. However, these technologies suffer from a range of disadvantages stretching from inefficiency to remove pollutants at low concentration and to completely convert pollutants into biodegradable or less toxic byproducts, high energy and chemicals consumption, process complexity, high maintenance and operation costs, etc. [9–11]. An efficient and viable treatment process should meet both economic and environmental requirements to be marketed

and applied in large scale. The incorporation of low-cost and available materials in different treatment processes could decrease the global treatment cost and increase the process efficiency.

Biochar as an eco-friendly and low-cost material generally produced from organic wastes such as agricultural wastes, forestry residues and municipal wastes has attracted increasing attention evidenced by its increasing use in different environmental applications. Organic wastes could be converted into char by different techniques including pyrolysis, hydrothermal carbonization (HTC), gasification, and torrefaction [12]. The conventional carbonization method for producing biochar is pyrolysis, while chars from gasification, torrefaction, and HTC generally do not meet the definition of biochar specified in the guidelines for the European Biochar Certificate (EBC). Owning to its enhanced properties such as rich carbon content, enhanced surface area, high cation/anion exchange capacity, and stable structure [13], biochar and its activated derivatives were reported as very efficient materials to remove various contaminants, including pathogenic organisms [14–17], inorganics such as heavy metals [18,19], and organic contaminants such as dyes [20,21]. This evidence is however derived only from batch experiments, while a lack of information on the design and optimization of biochar-based systems for the depollution of drinking water and the treatment of wastewater is still largely existing. The ability of biochar to remove organic and inorganic pollutants from wastewater is directly linked to its adsorption capacity, which depends on their physico-chemical characteristics such as elemental composition, surface area, distribution of pore size, surface functional groups, and cation/anion exchange capacity, these physico-chemical properties vary with the nature of feedstock and the preparation methods and conditions [22–25]. For some recalcitrant molecules, which are present at low concentrations, the properties of biochar should be modulated to allow for a better removal efficiency. The common methods used for biochar modification are regrouped into two classes: chemical modification methods, which mainly include acid modification, alkalinity modification, and oxidizing agent modification; and physical modification methods generally performed by gas purging.

Although biochar showed widespread application prospect in the wastewater remediation, the potential negative impact of biochar application should be also analyzed. Depending on the nature of feedstock and the conversion technique adopted for its production, biochar may contain various heavy metals and other contaminants that could be released during its application in aqueous solutions [26,27]. Therefore, more studies are needed to investigate the stability of biochar and its correlation with the experimental conditions used during biochar production. In this review, the recent studies on the preparation, modification and use of biochar from pyrolysis and chars from other thermal conversion processes for the removal of organic and inorganic wastewater pollutants are summarized. The main mechanisms involved during the adsorption process, in addition to the recent advancement in the application of biochar as filtration media, support for catalysts, and its role during anaerobic digestion of wastewater, will be also discussed.

2. Conventional Thermal Methods for the Conversion of Feedstock into Carbonaceous Materials

2.1. Pyrolysis

Pyrolysis is one of the main thermal processes used for converting organic wastes into carbonaceous materials that can be used for wastewater depollution [28,29]. During pyrolysis, lignin, cellulose, hemicellulose, and fat in the feedstock are thermally broken down in oxygen-free conditions to enrich the carbon content of the starting material by eliminating non-carbon species such as oxygen and hydrogen [30]. Carbonization temperature, heating rate, nitrogen flow rate, and carbonization time are the main factors controlling the process of pyrolysis and profoundly determine the nature and the distribution of carbonization products: biochar (solid fraction), bio-oil (small quantities of condensable liquid), and non-condensable gases (syngas) (e.g., CO, CO_2, CH_4, and H_2) [31,32]. The removal of different elements (carbon, hydrogen, oxygen) in the form of gases and volatiles results in a decrease in O/C and H/C atomic ratios and correspondingly an increase in aromaticity and carbon content, which enhances the biochar stability [33,34]. This tendency becomes more pronounced as the

pyrolysis temperature increases. Increasing pyrolysis temperature (>500 °C) results also in greater hydrophobicity and higher surface area and micropore volume [35], which make of the produced biochar highly amenable for the removal of organic pollutants. Lower pyrolysis temperature (<500 °C), however, allowed for a biochar with smaller pore size, lower surface area, and higher oxygen-containing functional groups [36], which was more suitable for the removal of inorganic pollutants. The increase in pyrolysis temperature also increases the pH of biochar due to the enrichment of ash content [34,37,38]. The heating rate is also an important factor that must be controlled during the process of carbonization. A high heating rate promotes the release of gases and the decrease in the solid yield [39]. Pyrolysis could be classified into slow and fast pyrolysis based on the temperature, heating rate, pressure, and residence time used during the process. Pyrolysis reaction conditions and associated by-products distribution are summarized in Table 1. During slow pyrolysis, moderate temperatures and longer residence time are used in absence of O_2, which results in high biochar yield (30%) following the increasing cracking reactions that reduce condensable liquid products [40]. Contrary, fast pyrolysis produces biochar with lower mass yield (12%) and promotes the formation of bio-oil (up to 75%) from biomass [41,42].

Table 1. Thermal conversion processes and products distribution [33,43–46].

Process	Temperature	Heating Rate	Residence Time	By-Products [%]		
				Biochar	Bio-Oil	Syngas
Fast pyrolysis	400–1000 °C	Very fast (~1000 °C/s)	<2 s	12	75	13
Slow pyrolysis	350–980 °C	Slow (<10 °C/min)	1 h	27–37	19–29	25–41
HTC	180–300 °C	Slow	1–16 h	50–80	5–20	2–5
Gasification	700–1500 °C	Moderate-very fast	10–20 s	10	5	85
Torrefaction	200–300 °C	Slow, (<10 °C/min)	~10–60 min	80	0	20

2.2. Hydrothermal Carbonization

HTC is one of the most attractive thermochemical conversion methods used for high energy density materials production. This method is well adapted to wet feedstock without need of an energy intensive drying step; it allows high conversion efficiency of biomass to a carbonaceous material with relatively high yield at low operation temperature [47]. During HTC, the biomass in the presence of a liquid is subjected to temperatures ranging from 180 °C to 300 °C at a pressure between 2 MPa to 10 MPa for several hours [48]. Different biomasses were submitted to HTC such as two-phase olive mill waste [49], beet root chips [50], starch and rice grains [51], maize silage [48], and even polyethylene and rubber wastes [52]. Other studies have investigated the HTC of fecal biomass [53], sewage sludge [54] and agricultural residues [55]. During HTC of biomass, a decrease in the pH is typically observed; this is reported to be due to the formation of a variety of organic acids such as acetic, levulinic, formic, and lactic acids, which promotes the acid-catalyzed reaction of organic compounds without the addition of acid [56,57]. The presence of liquid during HTC allows the acceleration of the carbonization process; since water behaves as a solvent and reaction medium that enhances hydrolysis of lignocellulosic biomass [45]. The pretreatment of biomass by HTC follows different mechanistic pathways, resulting in three phases: hydrochar (solid fraction), aqueous phase (mixture of bio-oil and water), and a small volume of gas (mainly CO_2). The distribution of HTC byproducts and the properties of the hydrochar is also governed by factors such as process temperature, residence time, pressure and water/biomass ratio [58,59]. The non-soluble carbonaceous hydrochar has generally a structure with spherical particles due to the broken fibrous lignocellulosic chain at some places [60]. Particles contain a hydrophobic part (aromatic ring) and a hydrophilic part, which envelops the first part (Figure 1). The first part consists of stable oxygen atoms which are in the form of ether, quinone, etc. While the second part contains oxygenated functional groups (hydroxyl, phenolic, carbonyl, carboxylic, ester, etc.) [61]. Depending upon the process conditions used, the major part of carbon contained in the starting feedstock is remained in the final hydrochar, while a considerable amount of inorganics is removed from the hydrochar and dissolved in the liquid phase [45,56]. HTC is considered

to be a promising method to convert biomass into materials with abundant oxygen-containing functional groups and porous structure, which is beneficial for the adsorption of contaminants from wastewater [45,56]. Various hydrochar materials, such as switchgrass hydrochar [62], poultry litter and swine solids hydrochars [63], cassava slag hydrochar [64], banana peels hydrochar [65], and fructose and phloroglucinol hydrochars [66] have been reported as excellent adsorbents for the removal of different inorganic and organic contaminants. In the study by Elaigwu et al. [67], the effectiveness of hydrochar obtained from HTC of *Prosopis africana* shells was compared to that of pyrolytic-biochar to remove Pb and Cd from aqueous solution. Results showed that HTC-hydrochar was more efficient in adsorbing metal ions as compared to biochar from pyrolysis. The same tendency was observed by Liu et al. [68], who reported that hydrochar from pinewood exhibits higher efficiency to adsorb Cu than pyrolysis-biochar prepared from the same feedstock. The higher adsorption of HTC-hydrochar is due to the presence of more functional groups and available activated sites on its surface [67,68]. The adsorptive capacity of hydrochar could be improved by the addition of some chemical agent (acids, alkalis and surfactants) during the hydrothermal process [69,70]. Reza et al. [71] used acetic acid and potassium hydroxide as acidic and basic agent to modify the pH of the process water (from 2 to 12) during HTC of wheat straw. The results showed that hydrochar produced at pH 2 has 2.7 times higher surface area than that produced at pH 12 and larger pore volume and pore size.

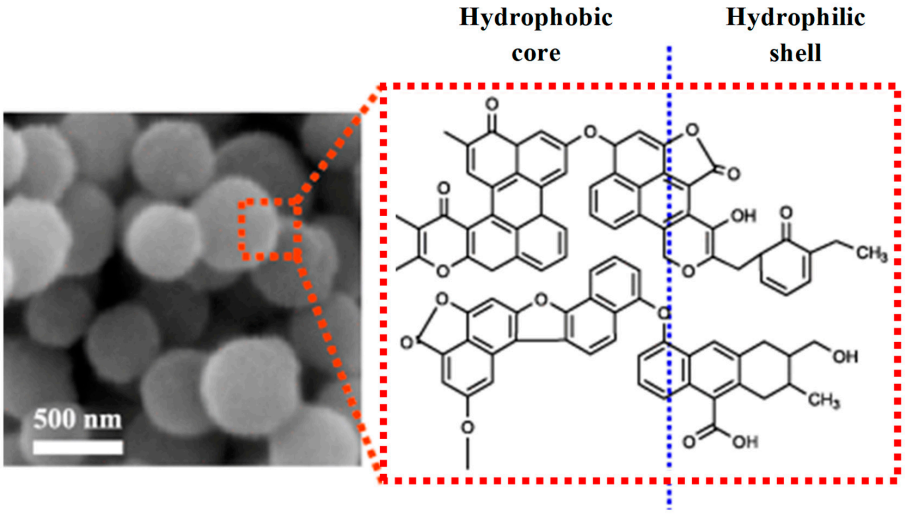

Figure 1. The microspheres core-shell structure of hydrochar. Reproduced from reference [61], Copyright (2009), with permission from John Wiley and Sons.

2.3. Gasification

Gasification is a thermochemical process performed by the conversion of biomass or other organic matter, into a gas mixture "syngas" (85%) containing H_2, CO, CO_2, and probably small hydrocarbons such as CH_4, a solid char (10%), and a liquid phase "tar" (5%) [72]. Tar and char are the undesirable byproducts of the gasification process. The properties of char generated from biomass gasification processes vary widely based on the nature of feedstock, reactor design, gasifying agent, and gasification temperature. In a study performed by Hernández et al. [73], the authors reported a low specific surface area (60 g/m^2) of char produced from gasification of dealcoholized marc of grape at 1200 °C under air flow, which discourages their application as activated carbon without further activation. However, García-García et al. [74] previously concluded that gasification of pine wood at 800 °C during 4 h under steam flow enabled the production of good quality activated carbon with a micropore volume of 0.263 cm^3/g and a surface area of 603 m^2/g. Equally, Galhetas et al. [75] tested the capacity of chars produced from gasification of coal and pine and activated with potassium carbonate to adsorb acetaminophen and caffeine from aqueous solutions. The authors reported that the highest porosity development was obtained with the char derived from pine after gasification at 850 °C under air flow

and activated with potassium carbonate at 800 °C during 2 h. The produced carbon material exhibited a mass yield of about 35% along with a high surface area of 1500 m^2/g and adsorption capacities of 434.8 mg/g and 476.2 mg/g toward acetaminophen and caffeine, respectively. Contrary to biochar prepared by pyrolysis that have been extensively explored, fewer studies evaluated the characteristics of char from biomass gasification. Nevertheless, a thorough knowledge of the char properties and its correlation with the gasification technology are crucial in the view of its potential valorization in water and wastewater decontamination.

2.4. Torrefaction

Torrefaction is a conventional thermal pretreatment of biomass performed to improve the physicochemical and thermochemical properties of biomass; it enables the energy densification and the homogenization of biomass. The torrefaction is performed generally at slow heating rates under atmospheric pressure at temperatures ranging from 200 °C to 300 °C and without or with limited oxygen supplies [76]. Torrefaction is dominantly used for biofuel production [77], while pyrolysis is the dominant process to prepare biochar for water and wastewater depollution. Compared to biochar, torrefaction-char may contain higher amount of oxygen-containing functional groups, attributed to the much lower temperatures used during the thermal process [77]. Thus, torrefaction-char might be used as an efficient adsorbent. Li et al. [78] compared between the physico-chemical properties of char prepared by torrefaction at 200–300 °C and biochar prepared by pyrolysis at 500 °C and their removal efficiencies toward U(VI) and methylene blue. The results showed that the maximum adsorption capacities towards U(VI) and methylene blue were increased, respectively, from 56.2 and 192.7 mg/g for biochar to >100 and >350 mg/g for torrefaction-char, indicating that char from torrefaction is much more efficient than biochar from pyrolysis for water pollution control. Torrefaction-char from barley straw produced at 220 °C during 20 min was also used as an adsorbent and showed enhanced adsorption capacity towards methylene blue [79]. Due to the lower process temperature, simpler preparation method, and higher product yield, the torrefaction-char as an oxygen-rich-char could be considered as a promising adsorbent. More attention should be paid for its application for contaminants removal.

3. Modification of Biochar

Owing to the little functional groups and the small surface area and pore volume exhibited by the biochar and the fact that in case of dry pyrolysis, the pores formed during carbonization are plugged with tarred material, a subsequent chemical or physical treatment is required to improve the properties of specific surface area, pore volume, and pore structure of the biochar for its subsequent use in different environmental applications.

During physical modification, biochar is subjected to a controlled gasification at high temperature and under activation atmosphere. Significant changes in textural characteristics including changes in surface area, pores volume and pores distribution and in surface chemical properties including surface functional groups, hydrophobicity, and polarity were observed after physical activation [80,81]. The widely oxidizing agent used for the biochar modification using the physical method is water steam. Chemical reactions involved during steam activation can be expressed as follows [82] (Equations (1) and (2)):

$$C + H_2O ==> CO + H_2 , H = 117 \text{ KJ/mol} \quad (1)$$

$$CO + H_2O ==> CO_2 + H_2 , H = 41 \text{ KJ/mol} \quad (2)$$

The steam activation process can selectively eliminate most reactive carbon atoms from the original biochar and then generate porosity and surface area. The reaction between steam and carbon induces an elimination of volatile materials and a decomposition of tar, which leads to the development of new micropores and the further widening of existing pores [83]. This tendency is more pronounced as the temperature increases [83]. However, at high temperatures, a significant decrease in mass yield was also observed, which does not allows the process to be economically favorable. Prolonged residence

time leads to the improvement of surface area and porous structure until a limit where further increase may induce a widening of existing pores with little new pore formation, which causes the reduction in surface area and pore volume. Steam flow rate, the nature of the precursor, and its composition could also be considered as factors effecting steam activation, but there still is a luck in information to figure out their in-depth influence mechanisms. The activation with steam generally favors carbon microporosity and leads to a final activated biochar with a well-developed microporosity with a very small contribution of mesoporosity [82]. Similar to steam modification, gas purging modification can also be applied to improve the structure of biochar and increase its surface area, thus enhancing its adsorption capacity. It consists of a first pyrolysis step of feedstock followed by a purging step of the biochar by carbon dioxide or ammonia gas. Carbon dioxide modification can promote the microporous structure of biochar, while ammonia gas modification introduces nitrogen-containing groups on the biochar [84]. The modification of cotton-stalk-derived biochar by a mixture of carbon dioxide and ammonia gas was reported by Zhang et al. [85] as more efficient to increase the biochar surface area compared with single modification using carbon dioxide or ammonia gas.

During chemical activation, biochar is impregnated with chemical agents such as acids (hydrochloric acid, nitric acid, sulfuric acid, and phosphoric acid), bases (potassium hydroxide, sodium hydroxide, and potassium carbonate), and oxidants (hydrogen peroxide and potassium permanganate). The acid modification aimed mainly to introduce acid functional groups on the surface of biochar. Peng et al. [86] modified reed-derived biochar by 1 M hydrochloric acid and reported an enrichment of hydrophobic adsorption sites for the adsorption of pentachlorophenol. Equally, Mahmoud et al. [87] reported that the treatment of kenaf fiber biochar by hydrochloric acid resulted in the increase of surface area of 289.5–346.6 m^2/g. giving favor to highly porous activated biochar showing a honeycomb with various sizes. Acid modification can also change the surface area and the pore structure of the biochar depending on the type and concentration of the acid [88]. Peng et al. [86] found that the use of 1 M of hydrochloric acid increased the surface area of biochar from 58.8 m^2/g to 88.4 m^2/g. While the modification of biochar by a combination of 30% sulfuric acid and oxalic acid induces a significant increase in the surface area from 2.3 m^2/g to 571 m^2/g [89]. Alkaline modification increases the surface area and the oxygen-containing functional groups on the surface of biochar. In the study carried out by Enaime et al. [28], authors activated biochar prepared from a mixture of olive solid wastes and olive mill wastewater using potassium hydroxide as an activating agent. The activated biochar showed high surface area (1375 m^2/g) and micropore volume (0.52 cm^3/g) and exhibited high adsorption capacity toward indigo carmine (599 mg/g). In another study, Jing et al. [90] modified municipal solid wastes–derived biochar by potassium hydroxide and showed an increase in the surface area from 14.4 m^2/g to 49.1 m^2/g and in the oxygen-containing functional groups on the biochar surface, which resulted in an enhancement of the As(V) removal efficiency. Contrary, a decrease in the surface area from 4.4 m^2/g to 0.69 m^2/g was reported by Shen and Zhang [91] by using potassium hydroxide for the modification of wheat-straw-derived hydrochar. As compared to potassium hydroxide, sodium hydroxide modification of coconut-derived biochar significantly increased its surface area up to 2885 m^2/g, which was higher than that reported for coconut shell derived biochar modified by potassium hydroxide (1940 m^2/g) [92]. The characteristics of the biochar modified by alkaline agents is strongly dependent on the types of feedstock and the preparation method. The ratio between base and biochar was also reported as significant factor affecting the properties of biochar [91].

In comparison between acid and basic treatments, Iriarte et al. [93] studied the effect of different agents (phosphoric acid, sulfuric acid, sodium hydroxide and potassium carbonate) on the properties of pork bone char. Results showed that sulfuric acid treatment produced biochar with high microporosity and the treatment with sodium hydroxide and potassium carbonate increased more the amounts of micropores and mesopores within biochar structure. While the effect of phosphoric acid on biochar was extremely aggressive and leads to a destruction of biochar pore structure. Other than acid and basic modification, the modification using oxidizing agents such as hydrogen peroxide and potassium

permanganate was also reported to increase the content of oxygen-containing functional groups on the biochar. Xue et al. [94] treated a hydrothermally produced hydrochar from peanut hull with hydrogen peroxide. The results showed an increase in the oxygen-containing functional groups on the hydrochar surfaces, while no enhancement in the surface area was observed, as also reported by Tan et al. [95]. Contrary, the modification of hickory-wood-derived biochar by potassium permanganate enhanced its surface area from 101 m^2/g to 205 m^2/g and then enhanced its adsorption capacity toward Pb, Cu, and Cd [96]. The modification of biochar by organic solvents was also used. Jing et al. [90] modified a municipal solid waste-derived biochar by methanol and reported an esterification between the carbonyl groups and the biochar, which resulted in a significant enhancement of adsorption capacity toward tetracycline [90]. However, the practical application of organic solvent could be limited by its high cost and its volatile characteristic.

4. Biochar as an Efficient Adsorbent for Organic and Inorganic Pollutants

4.1. Organic Pollutants

Biochar derived from different biomass have been intensively and effectively used as sorbents for organic contaminants in water and wastewater. The greatest concern of organic contaminants in aqueous solutions has been focused on phenols and dyes (Table 2). For instance, pyrolysis biochar derived from macroalgae have been effectively used to remove textile dyes (malachite green, crystal violet and Congo red), which are hardly degraded due to their stability to light and oxidizing agents, and resistance to aerobic digestion [20]. Other biochars derived from switchgrass at higher than normal pyrolysis temperatures were used to effectively remove methylene blue, orange G, and Congo red [21]. The results indicated that methylene blue (cationic dye) was highly adsorbed than orange G and Congo red (anionic dye), this was reported due to the small molecular weight of methylene blue and its favorable electrostatic property and strong π–π interaction with biochar surface. Adsorption was also high for biochars prepared at 900 °C than those prepared at 600 °C due to the significantly enhanced surface area at the highest pyrolysis temperature. Biochar have also been reported as an effective adsorbent for phenols in wastewater [97,98]. The study of Thang et al. [97] investigated the potential of biochar derived from chicken manure to remove toxic phenol and 2,4-dinitrophenol from aqueous solution. The obtained biochar exhibited higher adsorption capacities; 106.2 m^2/g for phenol and 148.1 mg/g for 2,4-dinitrophenol and a high stability up to five cycles. According to the authors, the interaction mechanisms such as hydrogen bonding, electrostatic interaction and π–π bonding are possibly interfering during the adsorption of phenols on biochar under various conditions [97]. In the study performed by Oh and Seo [99], polymer/ biomass-derived biochar was used for the removal of ionizable halogenated phenols from aqueous solution. Solution pH was an important factor in controlling the hydrophobicity and deprotonation of compounds, which was confirmed by correlation analysis of the maximum sorption capacity.

The effectiveness of straw-based biochar as compared to that of commercial activated carbon to remove dyes (reactive brilliant blue and rhodamine B) was evaluated by Qiu et al. [100]. Both carbon materials showed high affinity to adsorb reactive brilliant blue and rhodamine B at pH values of 3.0 and 6.5 with slight difference in favor of biochar to adsorb rhodamine B due to the enhancement of the π-π interactions by the surface functional groups of the biochar. In another study performed by Ferreira et al. [101], authors compared the adsorptive performance of biochars from paper mill sludge with commercial activated carbon to remove fish anaesthetics from water in recirculating aquaculture systems. Despite the higher adsorption capacity of the commercial activated carbon (289–631 mg/g) as compared to the biochars (53–109 mg/g), the authors concluded that paper mill sludge–based adsorbents could be considered as a cost-effective alternative for the adsorption of fish anaesthetics considering that the cost associated to the precursor (paper mill sludge) of these adsorbents is null and the production process did not use chemicals and allows the recovery of energy from wastes, which makes the whole process as an environmentally friendly process.

4.2. Heavy Metals

Recent studies showed that biochar offers an excellent ability to remove inorganic pollutants such as heavy metals from wastewater (Table 3). It has been widely recognized that the adsorption capacity of biochar toward heavy metals largely depends on biochar characteristics and the nature of the target metals [102–105]. Biochar can be an effective material for the sorption of heavy metals due to the abundance of functional groups on its surface such as phenolic, hydroxyl, and carboxyl groups, and due to its porous structure and its large surface area [106,107]. Jingjian et al. [108] compared between straws of canola, rice, soybean and peanut derived biochars for the adsorption of trivalent chromium. The adsorption capacities were consistent with the content of acidic functional groups of the biochars and vary in the following order peanut > soybean > canola > rice. In another study performed by Zhao et al. [107], the properties of biochars from rice straw, chicken manure, and sewage sludge and their effect on the removal efficiency of Pb^{2+} and Zn^{2+} were investigated. The highest carbon and hydrogen contents, the greatest number of functional groups (e.g., O-H and C=C/C=O), the highest pH, the most negative surface charge, and the highest physical stability were exhibited by the rice straw biochar, which also showed the highest adsorption capacity toward Pb^{2+}. Precipitation and ion exchange reactions have been widely considered as possible mechanisms for heavy metals adsorption. Park et al. [109] testing rice straw biochar for the removal of Cu^{2+} and Zn^{2+} reported that ion exchange of native cations with Cu^{2+} and Zn^{2+} cations is the dominant mechanism controlling the adsorption. Xu et al. [110] separated biochar into organic and inorganic fractions and tested their capacity in removing Pb. The Pb adsorption capacity of the inorganic fraction was higher than 300 mg/g, while the adsorption was only 1 mg/g for the organic fraction; this was reported to be due to the dominance of the cation exchange and Pb precipitation during the adsorption process, while Pb complexation with organic functional groups was limited [110]. In another study performed by Liu and Fan [111], rice straw-derived biochar was tested for the adsorption of Cd^{2+}. The results showed that minerals on the surface of the biochar containing Mg and Ca exchanged preliminary their cations with Cd^{2+}, which then form a precipitate within the biochar structure.

In comparison to other conventional adsorbents such as activated carbon, biochar could be a promising substitute for the adsorption of heavy metals. Kołodyńska et al. [112] reported that in spite of the lower surface area of biochar produced by gasification (115.5 m^2/g) in comparison to commercial activated carbon (759.8 m^2/g), the biochar removed more efficiently heavy metal ions from aqueous solutions than activated carbon. This was reported to be due to the type and the high amount of oxygen-functional groups on the biochar surface. Activation of biochar has been found to significantly improve its adsorption capacity toward heavy metals. Potassium hydroxide activated-biochar allowed for more than three-fold increase in the adsorption capacity of Cu^{2+} as compared to no-activated biochar [103]. Hydrochar from HTC of hickory and peanut hull was also physically activated by carbon dioxide, which significantly enhanced its adsorption capacity toward Pb^{2+}, Cu^{2+}, and Cd^{2+}. This was reported to be due to the improvement of the specific area of the hydrochar and to the introduction of acidic functional groups to its surface following the CO_2 activation which promoted the electrostatic attractions [113]. Samsuri et al. [114] studied the adsorption of AsV and AsIII by Fe-coated biochars from empty fruit bunch and rice husk. With Fe coating, the maximum AsIII sorption capacity increased from 19 mg/g to 31 mg/g, while AsV sorption increased from 5.5–7.1 mg/g to 15–16 mg/g. The reported sorption mechanism is through the complexation of AsV and AsIII with Fe on the biochar. The relatively high affinity of AsIII as compared to AsV could be due to the net charge of the biochar surface (negatively charged in the pH range of 2–9) and to the speciation of As in aqueous solution (AsIII mainly exists as H_3AsO_3 and AsV exists as $H_2AsO_4^-$ and $HAsO_4^{2-}$), which strongly depend on the pH value used during the adsorption experiment (8 for AsIII and 6 for AsV) [114]. Researchers have also focused their attention to understand the competitive adsorption of heavy metals on biochars and the mobility of single versus multiple heavy metal species [105,115]. In the study performed by Park et al. [105], sesame-straw-based biochar has been reported as more efficient in adsorbing metal in single metal systems than in a multi-metal system. Ni et al. [104] showed that the adsorption of

Pb^{2+} was more promoted than that of Cd^{2+} in a coexisting system, while in a single system Pb^{2+} ions are adsorbed on the same adsorption sites as Cd^{2+} ions. The hydrated ionic radius of the metal ion relative to the pore size plays an important role in competitive adsorption; as the hydrated ionic radius is small as the species are preferentially adsorbed compared to species with larger ionic radius [116]. Then, in addition to the biochar properties, the adsorption of heavy metals also depends on the nature of metals and their competitive behavior for biochar sorption sites.

4.3. Biochar Adsorption Mechanism

The biochar surface is characterized by its heterogeneity allowing for different sorption mechanisms to be occurred. The adsorption mechanism is depending on the nature of the contaminants and the chemical properties of the adsorbent surface [117]. According to Pignatello [118], the major routes of adsorption could be roughly divided into physical route where the adsorbate settles on the surface of the adsorbent, the precipitation route where the adsorbent form layers on the adsorbent surface and the porefilling route characterized by the condensation of the adsorbate into the pores of the adsorbent. For organic contaminants, the adsorption process is facilitated by electrostatic attraction, pore-filling, π-π electron-donor acceptor interaction, hydrogen-bonding, complexes adsorption, and hydrophobic interactions (Figure 2). For instance, the sorption of organic pollutants onto biochar by pore-filling is depending on the total micropore and mesopore volumes; the penetration of the pollutant on the biochar structure is more promoted as its ionic radius is low, which leads to an increase in the adsorption capacity of biochar [117,119]. Soluble pollutants can be attached to hydrophobic biochar when they have hydrophobic functional group or precipitated on alkaline biochar surfaces. The surface of biochar is usually negatively charged, due to the dissociation of oxygen-containing functional groups, which causes electrostatic attraction between biochar and positively charged molecules [119,120]. For biochar prepared at high temperatures the loss of oxygen-containing and hydrogen-containing functional groups make them less polar and more aromatic and then less appropriate for polar organic contaminants removal. However, the adsorption could occur by hydrogen-bonding promoted as a results of the electrostatic repulsion between negatively charged anionic organic compounds and biochar. The absence of hydrogen-bonding between water and oxygen-functional groups makes more pronounced the penetration of non-polar contaminant to hydrophobic sites [119]. For the removal of inorganic pollutants such as heavy metals, multitude mechanisms could interfere including surface precipitation under alkaline conditions, ion exchange and complexation, cationic and anionic electrostatic attraction (Figure 2). Lu et al. [121] studied the relative contribution of various mechanisms to Pb adsorption on sludge-derived biochar and proposed the following mechanisms: (i) electrostatic complexation due to metal exchange with cations (potassium and sodium) available in the biochar, (ii) co-precipitation and complexation with organic matter and mineral oxides of the biochar, (iii) surface complexation with free carboxyl and hydroxyl functional groups of the biochar, and (iv) surface precipitation as lead-phosphate-silicate ($5PbO.P_2O_5.SiO_2$).

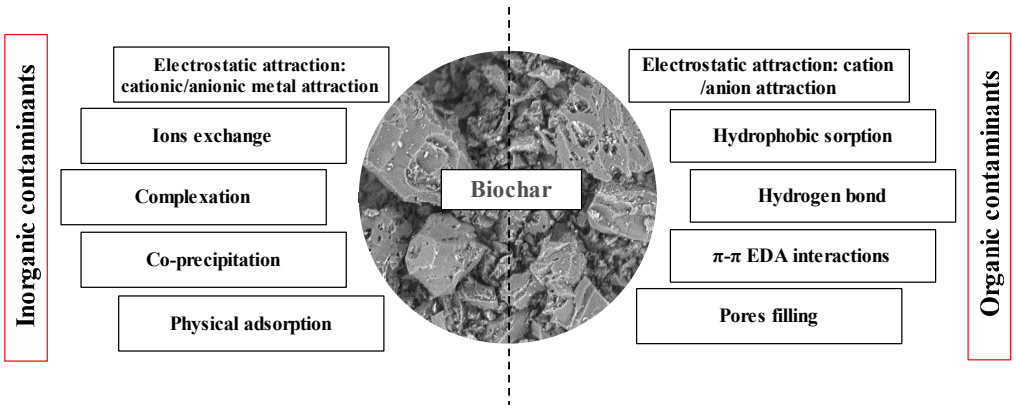

Figure 2. The proposed mechanisms for the removal of organic and inorganic contaminants by biochar.

Table 2. Physico-chemical properties of various chars produced from different feedstock and by different thermal conversion methods for dyes and phenols removal.

Feedstock	Preparation Conditions	Yield [%]	SAA [m^2/g]	Vt [cm^3/g]	Ash [%]	CEC [cmol/kg]	pH	Elemental Analysis [%]				Organic Pollutants	pH [a]	T [°C]	Q_{max} (mg/g)	Ref.
								C	H	N	O					
Pecan nutshell	Pyrolysis, 800 °C, 60 min	30	93	0.055	-	-	-	-	-	-	-	Reactive Red 141	3	35	130	[122]
Switchgrass	Pyrolysis, 450 °C, 20 min	-	-	-	-	-	-	-	-	-	-	Reactive red 195A	5	-	1288.4	[123]
Corn stalks	Pyrolysis, 400 °C, 120 min	-	-	-	-	-	-	-	-	-	-	Crystal violet	6	40	278.5	[124]
Macroalgae residue	Pyrolysis, 800 °C, 90 min	22.62	133.2	-	53.59		12.31	42.39	0.46	1.43	2.13	Malachite green	-	35	5306.2	[20]
												Crystal violet			1222.5	
												Congo red			345.2	
Durian rind	Pyrolysis, 800 °C, 25 min	-	820	-	-	-	-	-	-	-	-	Congo red	-	-	87.3	[125]
Switchgrass	Pyrolysis, 900 °C, 60 min	14.8	641.6	0.058	7.54	-	10.7	85.5	0.6	1.5	2.6	Methylene Blue	-	-	196.1	[21]
												Orange G	-	-	38.2	
												Congo Red	-	-	22.6	
Chicken manure	Pyrolysis, 500 °C, 120 min	-	68.8	-	-	-	-	54.3	10.5	4.5	18.8	Phenol	7	22	106.2	[97]
												2,4-Dinitrophenol			148.1	
Pine fruit shell	Slow pyrolysis, 550 °C, 60 min	29.23	228.11	0.148	3.23		8.7	83.27	3.69	0.00	13.04	Phenol	6.5	25	26.73	[98]
Rice straw	Pyrolysis, 500 °C, 60 min	28.0	96.0	0.06	50.1	-	-	-	-	-	-	Phenol	7	25	80.5	[126]
Rice husk	Pyrolysis, 650 °C, 60 min	34.1	21.7	-	36.0	-	-	60.3	0.1	0.4	37.6	Iodine	-	20	120.7	[127]
												Methylene blue			3.8	
Shore pine	Pyrolysis, 400 °C, 30 min	-	-	-	-	15.39	7.3	73.9	3.32	<0.5	-	Methylene blue	-	-	1.79	[128]
Sugarcane bagasse	Pyrolysis, 600 °C, 2 h and steam activation, 750 °C, 36 min	-	347.54	-	7.21	-	-	-	-	-	-	phenol	-	-	46.43	[129]
Pinewood sawdust	HTC, 300 °C, 20 min and activation, 800 °C, 1 h	53.8	425	-	2.90	-	-	-	-	-	-	phenol	-	-	83.88	[130]
Rice husk		80.5	358	-	59.96	-	-	-	-	-	-		-	-	39.30	
Barely straw	Torrefaction, 220 °C, 20 min	81.0	-	-	-	-	-	-	-	-	-	Methylene blue	-	23	11.65	[79]
Rice straw	Microwave assisted HTC, 180 °C, 50 min	42.31	15.9	-	22.13	-	-	40.06	5.52	0.48	31.79	Congo red	-	-	222.1	[131]
												Berberine hydrochloride	-	-	174.0	
Rice straw	Microwave assisted HTC 200 °C, 60 min	37.84	18.9	-	14.27	-	-	40.69	5.12	0.81	39.07	2-naphthol	-	-	48.7	[131]
Bamboo sawdust	HTC, 240 °C, 30 min	49.2	19.77	0.10	0.54			58.57	4.32	0.53	36.51	Congo red	-	25	96.9	[132]
												2-naphthol	-		462.6	
Chili seeds	HTC, 215 °C, 8 h	57.8	0.5	0.00457	-	-	-	64.04	7.58	1.70	26.60	Methylene blue	7	25	145	[133]
Walnut shell	HTC, 180 °C, 24 h	-	52.23	-	-	-	-	-	-	-	-	Methylene blue		25	68	[134]
Orange peles	HTC, 190 °C, 24 h	51.58	34.06	0.0474	-	-	-	78.85	-	1.23	19.92	Methylene blue	7	30	59.6	[135]
Rice husk	HTC, 260 °C, 60 min	28.1	3.5	-	2.7	-	-	73.3	4.9	2.7	19.0	Methylene blue	-	20	9.7	[127]
												Iodine	-		173.1	

Table 2. *Cont.*

Feedstock	Preparation Conditions	Yield [%]	SAA [m^2/g]	Vt [cm^3/g]	Ash [%]	CEC [cmol/kg]	pH	Elemental Analysis [%]				Organic Pollutants	pH [a]	T [°C]	Q_{max} (mg/g)	Ref.
								C	H	N	O					
Corn stover	Torrefaction, 250 °C, 0.5 h	-	-	-	30.38			42.92	2.39	1.55	22.25	Methylene blue			349.74	[78]
Olive wastes	Pyrolysis, 300 °C, 1 h and KOH activation, 850 °C, 1 h.	-	1375	0.84	-	-	-	-	-	-	-	Methylene blue	2	-	536	[28]
												Iodine			1136	
												Indigo carmine			598.8	
Coconut shell	Pyrolysis, 500 °C, 2 h and NaOH activation, 700 °C, 1.5 h.	18.8	2825	1.498	-	-	-	-	-	-	-	Methylene blue	-	-	916.26	[92]

[a] pH of the solution during the adsorption experiment; SSA: specific surface area; Vt: total pore volume; CEC: cation exchange capacity.

Table 3. Physico-chemical properties of various chars produced from different feedstock and by different thermal conversion methods for heavy metals removal.

Feedstock	Preparation Conditions	Yield [%]	SSA [m^2/g]	Vt [cm^3/g]	Ash [%]	CEC [cmol/kg]	pH	Elemental Analysis [%]				Metal	pH [a]	T [°C]	Q_{max} (mg/g)	Ref.
								C	H	N	O					
Rice straw	Pyrolysis 550 °C, 2 h	33.6	4.15	-	42.9	-	10.3	45.7	2.13	1.17	-	Pb^{2+}	5	25	0.85 [b]	[107]
												Zn^{2+}			0.61 [b]	
Chicken manure	Pyrolysis 550 °C, 2 h	77.5	7.09		87.2	-	9.95	7.49	0.43	0.76	-	Pb^{2+}	5	25	0.58 [b]	[107]
												Zn^{2+}			0.17 [b]	
Sewage sludge	Pyrolysis 550 °C, 2 h	79.0	8.20		68.7	-	7.62	18.9	1.70	2.92	-	Pb^{2+}	5	25	0.11 [b]	[107]
												Zn^{2+}			0.07 [b]	
Chestnut shell	Pyrolysis 450 °C, 2 h	-	-	-	-	-	-	-	-	-	-	As(V)	7	25	17.5	[88]
Canola straw	Pyrolysis 400 °C, 3 h 45 min	-	-	-	-	316.9	-	-	-	-	-	Cr(III)	4	25	0.28 [b]	[108]
Rice straw		-	-	-	-	483.1	-	-	-	-	-				0.27 [b]	
Soybean straw		-	-	-	-	229.5	-	-	-	-	-				0.33 [b]	
Peanut straw		-	-	-	-	196.2	-	-	-	-	-				0.48 [b]	
Almond shell	Pyrolysis 650 °C	-	145	-	-	-	-	-	-	-	-	Ni(II)	7	40	22.2	[136]
												Co(II)	7	20	28.09	
Coconut fiber	Pyrolysis, 300 °C, 6 h	-	4.495	-	3.76	72.86	7.41	-	-	-	-	Pb^{2+}	6	25	49.5	[137]
Pineapple peels	Pyrolysis, 350 °C, 1 h	-	-	-	-	-	-	-	-	-	-	Cr(VI)	2	30	41.7	[138]
Hardwood (Acacia)	Pyrolysis, 300–400 °C, 2 h	-	1.30	-	3.5	-	7.62	69.6	4.3	0.6	22.0	Cu^{2+}	5	-	3.48	[139]

Table 3. *Cont.*

Feedstock	Preparation Conditions	Yield [%]	SSA [m^2/g]	Vt [cm^3/g]	Ash [%]	CEC [cmol/kg]	pH	Elemental Analysis [%]				Metal	pH [a]	T [°C]	Q_{max} (mg/g)	Ref.
								C	H	N	O					
Hardwood (Citrus)	Pyrolysis, 300 °C	41.6	0.8	-	8.43	-	7.76	60.37	4.43	1.43	25.34	Pb^{2+}	-	22	7.153	[140]
Wheat Straw	Pyrolysis, 600 °C, 5 h	-	26.3	-	41.1	6.12 [c]	9.9	54	2.3	0.9	2.3	Cd^{2+}	5.5	22	17.92	[141]
												Ni^{2+}			16.26	
Rice Straw	Pyrolysis, 600 °C, 4 h	21.2	162.6	-	-	-	9.89	68.7	2.3	3.0	25.9	Zn^{2+}	5	25	38.6	[109]
												Cu^{2+}			56.5	
Rice husk	Pyrolysis, 650 °C, 1 h	34.1	21.7	-	36.0	-	-	60.3	0.1	0.4	37.6	Cu^{2+}	4.8	20	48.9	[127]
Anaerobically digested sludge	Pyrolysis, 600 °C, 2 h	52.6	162.7	0.04	-	-	-	27.8	1.3	-	9.6	Pb	7	22	0.61 [b]	[104]
Sugarcane bagasse	Pyrolysis, 300 °C, 20 min	-	-	-	-	-	-	-	-	-	-	Pb	6.3	25	53.48	[142]
Sugarcane bagasse	Pyrolysis, 500 °C	-	92.30	0.04531	12.21	-	9.63	74.02	2.61	1.00	22.37	Pb(II)	5	30	86.96	[143]
Orange peel		-	0.21	0.00016	11.17	-	8.75	66.36	3.60	2.13	28.09				27.86	
Macroalgae (Enteromorpha)	Hydrothermal liquefaction, 250 °C, 40 min	20.5	29.7	-	-	-	-	70.2	4.5	-	23.1	Cu^{2+}	8.1	-	0.254	[18]
												Pb^{2+}			0.098	
Sawdust	HTC, 190 °C, 12 h	-	7.86	0.61	-	-	-	60.78	6.02	0.94	32.26	Cu^{2+}	5	25	298.9	[144]
Rice husk	HTC, 260 °C, 1 h	28.1	3.5	-	2.7	-	-	73.3	4.9	2.7	19.0	Cu^{+2}	4.8	20	68.2	[127]
Banana peels	HTC, 230 °C, 2 h	15.6	31.65	-	0.53	-	-	71.38	6.34	0.57	19.78	Pb^{2+}	-	-	315.16	[65]
Rice Straw	Microwave assisted HTC 160 °C, 60 min	42.53	8.21	-	17.56	-	-	40.34	5.11	1.15	35.76	Cu^{2+}	-	-	144.9	[131]
Rice Straw	Microwave assisted HTC, 200 °C, 50 min	36.22	25.4	-	19.53	-	-	37.44	4.85	0.75	37.4	Zn^{2+}	-	-	112.8	[131]
Wood chips (pine and spruce)	Gasification at 1000 °C	-	14.4	0.03	-	-	-	-	-	-	-	Fe	4	-	24.1	[145]
												Cu	5		11.1	
												Ni	8		5.6	
Wood chips (pine and spruce)	Gasification at 1000 °C and $ZnCl_2$ activation, 500 °C, 1 h	-	259	0.26	-	-	-	-	-	-	-	Fe	-	-	20.5	[145]
												Cu			23.1	
												Ni			18.2	
Pinewood sawdust	HTC, 300 °C, 20 min and CO_2 activation, 800 °C, 1 h	53.8	425	-	2.90	-	-	-	-	-	-	Cu	-	-	25.18	[130]
Rice husk		80.5	358	-	59.96	-	-	-	-	-	-		-	-	22.62	

[a] pH of the solution during the adsorption experiment; [b] expressed in mmol/g; [c] expressed in meq/100 g; SSA: specific surface area; Vt: total pore volume; CEC: cation exchange capacity.

4.4. Parameters Affecting the Adsorption of Pollutants on Biochar

4.4.1. Biochar Characteristics

The sorption of an adsorbate by an adsorbent is controlled by its accessible volume of micropores [146,147]. Adsorbent materials contain pores of various sizes that are grouped into micropores, mesopores, and macropores based on the width of opening [148]. The size and distribution of pores is largely dependent on the experimental conditions used during biochar production with temperature having the greatest impact [149]. Micropores are reported as the most abundant within the biochar structure and the responsible for its surface area and its high adsorptive capacity. Zabaniotou et al. [147] reported that biochar produced by pyrolysis at high temperatures contains a high micropores volume that range between 50%–78% of the total pores. The size of the adsorbate is also an important parameter controlling the sorption rate of the biochar. While larger adsorbate size can cause exclusion or blockage of sorption sites, smaller particle sizes reduce the mass transfer limitation and increase the van der Waal force of penetration of the adsorbate into the adsorbent [150]. The adsorption rate of biochar also depends on types and levels of surface functional groups [120]. The distribution of surface functional groups is determined by the chemical composition of the feedstock, the carbonization method and the temperature of carbonization [31]. Gascó et al. [151] compared the properties of biochar and hydrochar obtained from pyrolysis and HTC of pig manure. Results showed that the broad peak at 3400 cm^{-1}, assigned to -OH stretching vibration in carboxyl and hydroxyl groups, becomes less obvious in biochars compared to the feedstock following the pyrolysis temperature increase. HTC-hydrochars also showed a broad band at 3400 cm^{-1} with lower intensity than for the feedstock due to dehydration and decarboxylation reactions occurred during the HTC process. Authors concluded that pyrolysis at high temperature (600 °C) produced biochars with high aromatic structure, while HTC process at 200–240 °C during 2 h give favor to biochar with increased amount of aliphatic structures. Qambrani et al. [120] stated that due to pyrolytic conditions, the O-H, -CH_2, CO=, CC=, and -CH_3 functional groups were altered in biochar, which promotes the biochar hydrophobic interactions. The abundance of oxygen- and nitrogen-containing functional groups determines the hydrophobic nature of biochars, the lower the oxygen- and nitrogen-containing functional groups in the biochar, the more hydrophobic the biochar [152]. Biochars with hydrophobic nature are believed to contribute in the adsorption of insoluble adsorbates, while hydrophylic biochar are reported as less effective due to the sorption of water; the presence of oxygen-containing functional groups on the hydrophilic biochar surface allows the penetration of water via hydrogen-bonding, which leads to a competitiveness between water and adsorbate for the available sites on the biochar surface [153]. In aqueous solutions, the insoluble or less soluble adsorbates are more likely to be adsorbed in the pores of the biochar [153].

4.4.2. Solution pH

The solution pH is an important factor that control the adsorption process by influencing the surface charge of the adsorbent and the speciation, the charge and the degree of ionization of the adsorbate [136]. When the solution pH is greater than the point of zero charge, negative charge exists on the surface of the adsorbent following the deprotonation of phenolic and carboxylic groups on its surface, then the competitiveness between the protons and the cation contaminants decreases. At lower pH, basic functional groups such as amine get protonated and possess a positive charge, which promoted the adsorption of anions [154–156]. This implies that the adsorption behavior of biochar is a function of the pH of the medium and the deprotonation of functional groups. The impact of pH on biochar adsorption capacity toward ammonium (NH_4^+-N) was demonstrated by Kizito et al. [157] and Hu et al. [158]. The authors showed that the adsorption of NH_4^+-N over biochar was lower when the pH was lower (e.g., pH = 3 or 4). With the increase in initial solution pH between 4 and 8, the adsorption capacity of NH_4^+-N increased and then decreased again as the pH was higher than 9.

4.4.3. Adsorbent Dosage

The adsorbent dosage also has a profound influence on the sorbent-sorbate equilibrium of an adsorption system. The application of an increased adsorbent dosage increased the removal efficiency of organic and inorganic pollutants due to the availability of more sorption sites [159,160]. A reduction of the biochar adsorption capacity, however, could be observed when the dosage rate is in excess, consequently an overlapping of the adsorption layers could be occurred, which shields the available active sites on the absorbent surface [157,161]. The adsorbent dosage must be optimized to reach the high removal efficiency and to make the process cost-effective.

4.4.4. Temperature

The adsorption capacity of biochar has been reported to also be affected by the temperature of the medium in which it is applied. Most studies reported that the adsorption efficiency increased when the temperature raised showing an endothermic nature of the adsorption process. In the study performed by Enaime et al. [28], the authors reported that the sorption of indigo carmine onto potassium hydroxide activated biochar increases with the increase in the temperature due to the endothermicity of the sorption process. An increase in temperature produces an increase in the mobility of dye molecule and a possible increase in the porosity of the adsorbent. This may be due, also, to the swelling effect on the internal structure of adsorbent with increasing temperature, which allows more dye to penetrate further [162]. In another study, Kizito et al. [157] showed that the increase in the experimental temperature for the adsorption of NH_4^+-N from 15 °C to 45 °C allowed for an increase in the adsorption efficiency. They claimed that the raise of temperature above 30 °C to a maximum of 45 °C is beneficial for a maximum removal efficiency.

5. Environmental Application of Biochar for Wastewater Treatment

5.1. As a Support Media during Anaerobic Digestion

Anaerobic digestion is one of the most promising treatment technologies considered as an eco-friendly process for wastes management because of its ability to combine bioremediation and energy recovery. Performing the anaerobic digestion process under stable conditions with high energy recovery and efficient pollutants removal is a major concern for scientists since some constituents of the feedstock or their metabolic intermediate products could inhibit microorganisms and hinder their activity. Different approaches have been proposed so far to counteract the inhibition in anaerobic reactors such as the acclimation of bacterial cells, the adoption of thermophilic operating conditions and the reduction of the concentration of inhibitors either by dilution or by co-digestion with other substrates. The use of packing materials in anaerobic digestion has been proved as an advantageous alternative to reduce the mobility or bioavailability of inhibitors while allowing for the development of a large bacterial biomass within the digester.

Biochar as a porous, bio-stable, and available material has earned an increasing interest as an alternative to adsorbents like activated carbon and zeolite, and its application in anaerobic digestion is gradually increasing [163]. Moreover, the residual biochar in digestate can be directly reused as amendment to improve the soil properties without environmental risk [164]. The sorption capacity of biochar toward different organic and inorganic contaminants has been widely reported in the literature, but a lack of information with regard to its behavior toward inhibitory compounds during anaerobic digestion still exists. Mohan et al. [22] showed that biochar can adsorb NH_4^+ and remain stable in ambient air. Equally, Lü et al. [165] reported that biochar mitigates NH_4^+ inhibition during anaerobic digestion of glucose solution at an NH_4^+ concentration of 7 g/L. Torri and Fabbri [166] performed batch tests to investigate the anaerobic digestion of aqueous pyrolysis liquid. The results showed poor performance of the anaerobic process and underlined the inhibition of biological process even with the nutrient supplementation, whereas it was found that the biochar addition increased the yield of CH_4 and improved the reaction rate. In another study, Sunyoto et al. [167] investigated

the effect of biochar addition on H_2 and CH_4 production in a two-phase batch anaerobic digestion set-up. Their results showed that biochar addition increased H_2 and CH_4 yields and enhanced volatile fatty acids generation during H_2 production and VFAs degradation during CH_4 production. Compared to zeolite, Mumme et al. [168] reported that biochar showed less process stabilizing capacity. According to the same authors, further optimization can be assumed for the effective use of chars in anaerobic digestion.

The addition of biochar to increase the buffering capacity within digesters is another option that make beneficial the application of biochar during anaerobic digestion process. The acidification of digesters is often prevented by the addition of alkaline agents such as lime. However, some studies showed that the continuous addition of alkaline biochar could increase the buffering capacity of the anaerobic system [169,170]. Luo et al. [164] compared biochar and non-biochar incubation using glucose as a substrate and showed that for the tests performed by biochar, the CH_4 yield increased by about 90% while the acidification is reduced. Equally, Sunyoto et al. [167] reported that in addition to supporting microbial metabolism and growth, the application of biochar also buffered pH during biohydrogen production. The alkalinity of biochar is depending on the biomass source as well as on the carbonization temperature, with the alkalinity of biochar increases as the pyrolysis temperature raised [38,171].

The immobilization of biomass on a packing material that provides a very large surface area for microbial growth has been proved as an advantageous alternative, since it allows developing a large bacterial biomass that can be maintained within the reactors for a very long operation time, facilitating electron transfer between interspecies and reducing the distance between syntrophic bacteria and methanogens [172–176]. This can be beneficial to reduce the process start-up time, to assure better stability and higher tolerance toward high loading rates, and to allow for microorganisms to recover their performance very quickly after a period of starvation [177]. Packing materials such as zeolite, clay, activated carbon, and other plastic materials have been used to support microbial attachment and growth [174,178–181]. The application of biochar for cell immobilization is, however, not as extensive as most other adsorbents. In a study performed by Sunyoto et al. [182], the authors reported that biochar promoted the methanogenic biofilm formation, which enhanced the microbial activity, volatile fatty acids degradation and CH_4 production. Luo et al. [164] observed the colonization of *Methanosarina* on biochar material during anaerobic digestion of glucose. The authors showed that the use of biochar leads to an increase in biogas production by about 86% with a simultaneous enhancement of the degradation of intermediate acids as compared to the non-biochar study. The different studies performed so far, showed that the addition of biochar increases microbial metabolism and growth and provides favorable support for microorganisms [165,167]. However, no specific description on the special distribution of microorganisms on the biochar surface and the relationship between biochar structure and the amount of the immobilized microorganisms is provided.

5.2. As a Filtration Support Media

Biochar can be used in various water treatment designs. For instance, it can be incorporated in a biochar layer/column to a slow sand filter or bio-sand filter systems for the treatment of wastewater. The use of biochar filtration systems has received greater attention for its potential to remove particulate matter, heavy metals and reduce pathogen loads (Table 4). In a study performed by Kaetzl et al. [17], a higher removal efficiency of a *Miscanthus* biochar filter was observed, which was better or equal compared to a sand filter. Mean removal of chemical oxygen demand of biochar filter (74 ± 18%) was significantly higher than that of sand filter (61 ± 12%). The biochar filter also showed higher removal of *E. coli* with a mean reduction of 1.35 ± 0.27 log-units compared to that of sand filters with a mean reduction of 1.18 ± 0.31 log-units. Reddy et al. [14] evaluated the potential use of biochar as a filter media for the removal of total suspended solids, nutrients, heavy metals, and *E. coli* from synthetic storm water. The filtration on biochar was able to remove about 86% of suspended solids, 86% of nitrate and 47% of phosphate from the storm water effluent. After filtration, the concentration of Cd,

Cr, Cu, Pb, Ni, and Zn (heavy metals) were also reduced by 18, 19, 65, 75, 17, and 24%, respectively, while only 27% removal efficiency of *E. coli* was observed. This percentage was much lower than those reported for zeolite [183] and activated carbon [184], showing removal efficiencies of *E. coli* from storm water of about 53% and 98%, respectively. According to the authors, this difference could be due to the inflow concentration and the antecedent microbial levels as also reported by Chandrasena et al. [185].

The removal of suspended solids and organic matter in an anaerobic biochar filter, could be performed by a successive of steps, as described by Kaetzl et al. [186] (Figure 3), starting with a coagulation of suspended solids in the supernatant water layer followed by the sedimentation and the filtration of larger particles on the filter surface, smaller particles are removed by straining and adsorption in deeper filter zones, while organic matter is hydrolyzed under anaerobic conditions. The efficiency of the biochar filter increases with the increase in the surface area and the attachment sites on the biochar surface, which also support the biofilm establishment and the bacterial deposition within the filter column [186,187]. The reduction of pathogens could be governed by different key mechanisms including the filtration of larger pathogens (e.g., protozoa, amoeba) and the adsorption of negatively charged viral and bacterial cells. Other mechanisms such as the electrostatic attraction of bacteria to the biological film developed on the surface of the biochar filter [188] and the attachment of *E. coli* to the biochar filter coupled with the increase in the water-holding capacity could interfere. The biochar after filtration becomes enriched with nutrients and therefore can be reused as a fertilizer for soil amendment. In the study performed by Werner et al. [189], the biochar filter showed the same removal of pathogens as a common sand filter (1.4 log units on average). The concentration of P, Mg, and K were reduced during filtration, while N content remained unchanged. The agronomic effects of the biochar filter on spring wheat biomass production on an acidic sandy soil was evaluated. The results showed higher wheat biomass production for biochar filter (37%) treatment (20 t/ha), compared to the unamended control [189].

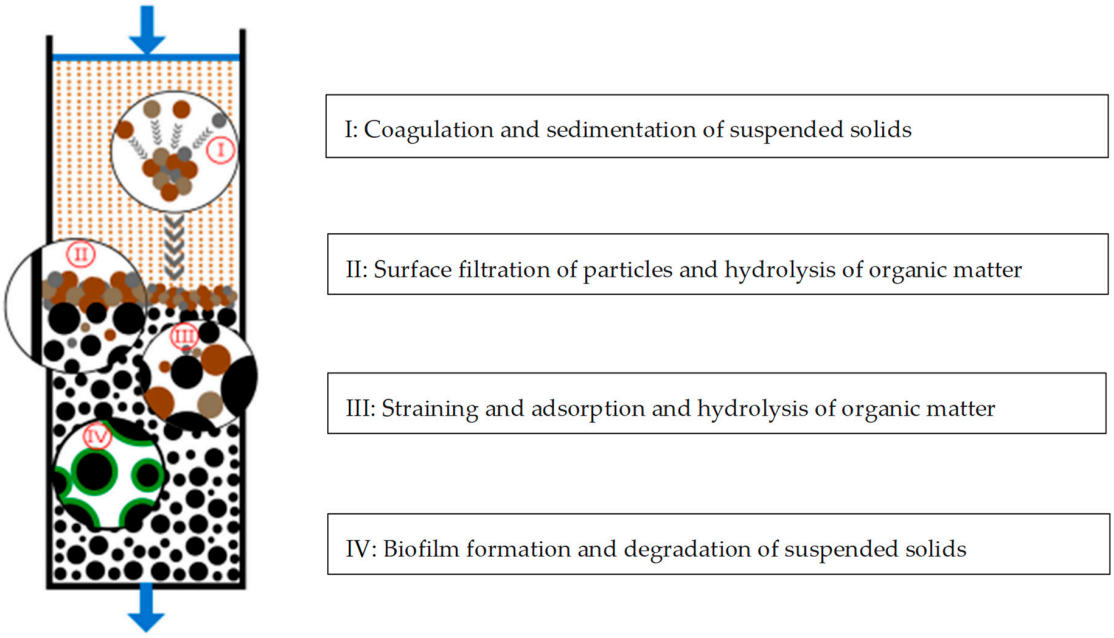

Figure 3. Estimated removal mechanism in an anaerobic biofilter using rice husk biochar as biofilter material. Reproduced from reference [186], copyright (2019), with permission from Elsevier B.V.

Table 4. Performance of different biochar filters used in the literature to remove pollutants from wastewater.

Feedstock	Preparation Conditions	Biochar Characteristics						Removal Efficiency				Ref.
		SSA [m^2/g]	Porosity [%]	C [%]	H [%]	O [%]	COD [%]	Nutrients [%]	TSS/Turbidity [%]	HM [%]	*E. coli* [%]	
Waste wood pellets	Gasification, 520 °C	-	-	-	-	-	-	NO_3-N: 86 Tot-P: 47	86	17–75	27	[14]
Miscanthus	Pyrolysis, 850 °C, 30 min	500	-	80.0	1.3	8.1	74	NH_4-N: ≈ 7 Tot-P: 35	31	-	23	[17]
Hard wood	-	184	72–74	-	-	-	95	Tot-N: 52 Tot-P:57	-	-	-	[190]
Pine-spruce	-	170–200	72–74	-	-	-	> 90	Tot-N: 50–52 Tot-P: 60–93	-	-	-	[191]
Forestry wood waste	Pyrolysis, 700 °C, 15 h	137.0	-	-	-	-	-	-	-	-	92–99	[192]
Rice husk	Gasification	143	-	-	-	-	94	Tot-N: 10.8 Tot-P: 5.3	63	-	55	[186]
Softwood	Pyrolysis, 815–1315 °C, 1–3 s	-	-	79	-	-	-	-	-	-	~96	[193]

SSA: Specific surface area; HM: heavy metals; COD: chemical oxygen demand; TSS: total suspended solids; NO_3-N: nitrate nitrogen; NH_4-N: ammonia nitrogen; Tot-N: total nitrogen; Tot-P: total phosphorous.

5.3. As a Catalyst during Heterogenous Oxidation

Biochar-based catalysts have been widely used in different systems for the degradation of biorecalcitrant compounds and the remediation of contaminants in wastewater, including catalytic ozonation processes, Fenton like reactions, and photocatalytic systems. Moussavi et al. [194] tested the catalytic potential of a biochar prepared from pistachio hull biomass and presented a macroporous structure and hydroxyl and phenolic surface functional groups for the ozonation of a water recalcitrant contaminant (reactive red 198 dye). Higher catalytic efficiency was exhibited by the prepared biochar at a pH of 10.0, with a catalytic potential of about 58% and a dye solution mineralization of 71% after a reaction time of 1 h. The excellent ability of carbon materials to activate various oxidants, such as oxygen and hydrogen peroxide, and form reactive oxygen species for the degradation of refractory organic contaminants has been widely reported in the literature [195–197]. Fang et al. [198] demonstrated that biochars originated from pine needles, wheat, and maize straw can induce OH generation in the presence of oxygen. Authors reported that free radicals in biochar transfer electrons to oxygen to form superoxide radical anion and hydrogen peroxide, which reacts further with free radicals to produce $^{\cdot}$OH, OH generated from biochar suspensions was found very efficient to degrade organic contaminants. Qin et al. [199] found that the hydrochar prepared by HTC enhanced Alachlor degradation in the Fe(III)/hydrogen peroxide Fenton–Like reaction by promoting Fe(III)/Fe(II) cycling via electron transfer from biochar to Fe(III). In another study performed by Izghri et al. [200], hydrochars were prepared by HTC of two-phase olive mill wastes impregnated with ferric chloride and used as catalysts for the degradation of methylene blue. The results showed that the hydrochar prepared at 250 °C HTC temperature during 4 h and with the ratio of ferric chloride to biomass of 1.5 has been effectively used as a catalyst in heterogeneous Fenton–Like oxidation, allowing for a degradation efficiency of methylene blue of about 91%.

6. Future Perspectives and Environmental Concern of Biochar

Biochar is a renewable resource that has significant potential to address several environmental issues in the field of wastewater depollution. Biochar is utilized as an adsorbent with high adsorbing capacity for a wide range of contaminants, however the detailed understanding of the different mechanisms governing the adsorption process are still lacking [201]. Since the efficient utilization of biochar for wastewater depollution depends on the biochar properties such as functional groups and surface area, on the availability and the nature of feedstock and on the conditions of thermal conversion method adopted for the biochar production, further studies are needed to center around "tuning" the biochar properties for tailored applications. Biochar modification is another important area that has to be exploited to enhance the biochar capacity for the removal of specific contaminants. Further research studies are needed to identify various modification methods and the different mechanisms involved according to the modification agents used. The understanding of the relationship between thermal conversion conditions, biochar properties, and biochar behavior toward wastewater contaminants can encourage its use for very complex compounds that hinder for example biological processes adopted for wastewater treatment. Thus, biochar could be incorporated in the pretreatment processes adopted to remove toxic compounds for subsequent biological treatment. Along with the wide application of biochar in the wastewater treatment field, scientists should pay attention to its potential negative effect on the environment. The stability of biochar is one of the most important properties that has to be taken into consideration when biochar is used. The stability of biochar refers generally to its aromaticity and degree of aromatic condensation [202]. When biochar is used for wastewater decontamination, the potential release of carbon from the biochar can increase the carbon content in the solution to be treated. In addition, a release of heavy metals could also occur, especially for biochar derived from sludge. Huang et al. [203] showed that the dissolution of organic matter from biochar into the aqueous solution is due to the biochar instability. The stability of the biochar was also found usually decreased after several cycles when the biochar is used as a support for catalyst due to the variation in the carbon structure of the biochar. The stability of biochar generally depends on the nature of the starting

feedstock and on the experimental conditions used during its thermal conversion. Thus, it is necessary to identify the correlation between these two parameters and the biochar stability. Another important factor is the regeneration and the recovery of biochar after use. The adsorption process is generally consisting of the transformation of pollution from the liquid phase to the solid material/adsorbent. Thus, it is important to convert the toxic pollutants that are bound with the biochar into a non-toxic state for their efficient management [159,204].

7. Conclusions

The low cost of feedstock and the simple preparation process combined with the enhanced physico-chemical properties of biochar make its application more feasible for wastewater treatment. This review systematically presented an overview of different biochar production techniques, adsorption mechanisms toward organic and inorganic contaminates, and prospective applications in the field of wastewater decontamination. The capacity of biochar to remove pollutants in aqueous solutions is directly linked with their physico-chemical properties, which depends on the nature of the starting feedstock, the thermal conversion technique, and the preparation conditions. The modification of biochar through physical and chemical activation methods was reported to adjust the functional groups on the surface of biochar, enhance its surface area and porous structure, and increase its surface oxygen-containing groups. Due to its unique and highly versatile characteristics, biochar has been effectively used in a variety of applications aiming the remediation of contaminated wastewater, including the adsorption of toxic heavy metals and dyes from the aqueous solutions, as a support for catalysts, as an immobilization support media for microorganisms and adsorbent of inhibitive compounds during anaerobic digestion. Overall, it is undoubted that the application of biochar offers several benefits and potential economic and environmental advantages, and its efficiency to remove different contaminants in the lab-scale has been widely reported. However, more in situ experiments should be performed to test the biochar efficiency using real effluents and to examine the real effect of biochar on the environment prior to its large-scale application. The stability of biochar after several cycles of use and its regeneration needs to be further investigated.

Author Contributions: Conceptualization, G.E. and M.L.; Section 1, G.E.; Section 2, G.E., A.B., M.L. and A.Y.; Section 3, A.Y. and A.B.; Section 4, G.E., M.L., A.B. and A.Y.; Section 5, G.E., M.L. and A.Y.; Section 6, G.E. and M.L.; Original draft preparation, G.E.; Revision of the draft manuscript, M.L. All authors have read and agreed to the published version of the manuscript.

Funding: This research received no external funding.

Conflicts of Interest: The authors declare no conflict of interest.

References

1. Zulfiqar, M.; Samsudin, M.F.R.; Sufian, S. Modelling and optimization of photocatalytic degradation of phenol via Tio_2 nanoparticles: An insight into response surface methodology and artificial neural network. *J. Photoch. Photobio. A* **2019**, *384*, 112039. [CrossRef]
2. Ayman, A.I.; Yahya, S.A.; Mohammad, A.A.; Amal, A.M.O. Studying competitive sorption behavior of methylene blue and malachite green using multivariate calibration. *Chem. Eng. J.* **2014**, *240*, 554–564.
3. Bogusz, A.; Oleszczuk, P.; Dobrowolski, R. Application of laboratory prepared and commercially available biochars to adsorption of cadmium, copper and zinc ions from water. *Bioresour. Technol.* **2015**, *196*, 540–549. [CrossRef] [PubMed]
4. Sadat, M.; Hashemi, H.; Eslami, F.; Karimzadeh, R. Organic contaminants removal from industrial wastewater by CTAB treated synthetic zeolite Y. *J. Environ. Manag.* **2019**, *233*, 785–792.
5. Vunain, E.; Masoamphambe, E.F.; Mpeketula, P.M.G.; Monjerezi, M.; Etale, A. Evaluation of coagulating efficiency and water borne pathogens reduction capacity of *Moringa oleifera* seed powder for treatment of domestic wastewater from Zomba, Malawi. *J. Environ. Chem. Eng.* **2019**, *7*, 103–118. [CrossRef]

6. Guillossou, R.; Roux, J.L.; Mailler, R.; Pereira-Derome, C.S.; Varrault, G.; Bressy, A.; Vulliet, E.; Morlay, C.; Nauleau, F.; Rocher, V.; et al. Influence of dissolved organic matter on the removal of 12 organic micropollutants from wastewater effluent by powdered activated carbon adsorption. *Water Res.* **2020**, *172*, 115487. [CrossRef]
7. Ejraei, A.; Aroon, M.A.; Saravani, A.Z. Wastewater treatment using a hybrid system combining adsorption, photocatalytic degradation and membrane filtration processes. *J. Water Process. Eng.* **2019**, *28*, 45–53. [CrossRef]
8. Nharingo, T.; Moyo, M. Application of *Opuntia ficus-indica* in bioremediation of wastewaters. A critical review. *J. Environ. Manag.* **2016**, *166*, 55–72. [CrossRef]
9. Cheng, Z.; Fu, F.; Dionysiou, D.D.; Tang, B. Adsorption, oxidation, and reduction behavior of arsenic in the removal of aqueous As(III) by mesoporous Fe/Al bimetallic particles. *Water Res.* **2016**, *96*, 22–31. [CrossRef]
10. He, J.; Li, Y.; Cai, X.; Chen, K.; Zheng, H.; Wang, C.; Zhang, K.; Lin, D.; Kong, L.; Liu, J. Study on the removal of organic micropollutants from aqueous and ethanol solutions by HAP membranes with tunable hydrophilicity and hydrophobicity. *Chemosphere* **2017**, *174*, 380–389. [CrossRef]
11. Fu, F.; Wang, Q. Removal of heavy metal ions from wastewaters: A review. *J. Environ. Manag.* **2011**, *92*, 407–418. [CrossRef] [PubMed]
12. Meyer, S.; Glaser, B.; Quicker, P. Technical, economical, and climate-related aspects of biochar production technologies: A literature review. *Environ. Sci. Technol.* **2011**, *45*, 9473–9483. [CrossRef] [PubMed]
13. Rizwan, M.; Ali, S.; Qayyum, M.F.; Ibrahim, M.; Ziaurrehman, M.; Abbas, T.; Ok, Y.S. Mechanisms of biochar-mediated alleviation of toxicity of trace elements in plants: A critical review. *Environ. Sci. Pollut. Res.* **2016**, *23*, 2230–2248. [CrossRef] [PubMed]
14. Reddy, K.R.; Xie, T.; Dastgheibi, S. Evaluation of biochar as a potential filter media for the removal of mixed contaminants from urban storm water runoff. *J. Environ. Eng.* **2014**, *140*. [CrossRef]
15. Molaei, R. Pathogen and Indicator Organisms Removal in Artificial Greywater Subjected to Aerobic Treatment. Master's Thesis, Department of Energy and Technology, The Swedish University of Agricultural Science in Uppsala, Uppsala, Sweden, February 2014.
16. Kaetzl, K.; Lübken, M.; Gehring, T.; Wichern, M. Efficient low-cost anaerobic treatment of wastewater using biochar and woodchip filters. *Water* **2018**, *10*, 818. [CrossRef]
17. Kaetzl, K.; Lübken, M.; Nettmann, E.; Krimmler, S.; Wichern, M. Slow sand filtration of raw wastewater using biochar as an alternative filtration media. *Sci. Rep.* **2020**, *10*, 1229. [CrossRef]
18. Yang, W.; Wang, Z.; Song, S.; Han, J.; Chen, H.; Wang, X.; Sun, R.; Cheng, J. Adsorption of copper(II) and lead(II) from seawater using hydrothermal biochar derived from *Enteromorpha*. *Mar. Pollut. Bull.* **2019**, *149*, 110586. [CrossRef]
19. Gwenzi, W.; Musarurwa, T.; Nyamugafata, P.; Chaukura, N.; Chaparadza, A.; Mbera, S. Adsorption of Zn^{2+} and Ni^{2+} in a binary aqueous solution by biosorbants derived from sawdust and water hyacinth (*Eichhornia crassipes*). *Water Sci. Technol.* **2014**, *70*, 1419–1427. [CrossRef]
20. Chen, Y.; Lin, Y.-C.; Ho, S.-H.; Zhouc, Y.; Ren, N. Highly efficient adsorption of dyes by biochar derived from pigments-extracted macroalgae pyrolyzed at different temperature. *Bioresour. Technol.* **2018**, *259*, 104–110. [CrossRef]
21. Park, J.-H.; Wang, J.J.; Meng, Y.; Wei, Z.; DeLaune, R.D.; Seo, D.-C. Adsorption/desorption behavior of cationic and anionic dyes by biochars prepared at normal and high pyrolysis temperatures. *Colloids Surf. A Physicochem. Eng. Asp.* **2019**, *572*, 274–282. [CrossRef]
22. Mohan, D.; Sarswat, A.; Ok, Y.S.; Pittman, C.U., Jr. Organic and inorganic contaminants removal from water with biochar, a renewable, low-cost and sustainable adsorbent: A critical review. *Bioresour. Technol.* **2014**, *160*, 191–202. [CrossRef] [PubMed]
23. Gai, X.; Wang, H.; Liu, J.; Zhai, L.; Liu, S.; Ren, T.; Liu, H. Effects of feedstock and pyrolysis temperature on biochar adsorption of ammonium and nitrate. *PLoS ONE* **2014**, *9*, e113888. [CrossRef]
24. Joyce, S.C.; Suzanne, B.; Ted, M.K.; Joseph, M.; Cliff, T.J.; Brad, J. Initial biochar properties related to the removal of As, Se, Pb, Cd, Cu, Ni, and Zn from an acidic suspension. *Chemosphere* **2017**, *170*, 216–224.
25. Brassard, P.; Godbout, S.; Raghavan, V. Soil biochar amendment as a climate change mitigation tool: Key parameters and mechanisms involved. *J. Environ. Manag.* **2016**, *181*, 484–497. [CrossRef] [PubMed]
26. Kim, J.H.; Ok, Y.S.; Choi, G.H.; Park, B.J. Residual perfluorochemicals in the biochar from sewage sludge. *Chemosphere* **2015**, *134*, 435–437. [CrossRef] [PubMed]

27. Jin, J.; Li, Y.; Zhang, J.; Wu, S.; Cao, Y.; Liang, P.; Zhang, J.; Wong, M.W.M.H.; Shand, S.; Christie, P. Influence of pyrolysis temperature on properties and environmental safety of heavy metals in biochars derived from municipal sewage sludge. *J. Hazard. Mater.* **2016**, *320*, 417–426. [CrossRef]
28. Enaime, G.; Ennaciri, K.; Ounas, A.; Baçaoui, A.; Seffen, M.; Selmi, T.; Yaacoubi, A. Preparation and characterization of activated carbons from olive wastes by physical and chemical activation: Application to indigo carmine adsorption. *J. Mater. Environ. Sci.* **2017**, *8*, 4125–4137.
29. Selmi, T.; Sanchez-Sanchez, A.; Gadonneix, P.; Jagiello, J.; Seffen, M.; Sammouda, H.; Celzard, A.; Fierro, V. Tetracycline removal with activated carbons produced by hydrothermal carbonisation of Agave americana fibres and mimosa tannin. *Ind. Crops Prod.* **2018**, *115*, 146–157. [CrossRef]
30. Islam, M.A.; Auta, M.; Kabir, G.; Hameed, B.H. A thermogravimetric analysis of the combustion kinetics of karanja (*Pongamia pinnata*) fruit hulls char. *Bioresour. Technol.* **2016**, *200*, 335–341. [CrossRef]
31. Ahmad, M.; Lee, S.S.; Dou, X.; Mohan, D.; Sung, J.K.; Yang, J.E.; Ok, Y.S. Effects of pyrolysis temperature on soybean stover and peanut shell-derived biochar properties and TCE adsorption in water. *Bioresour. Technol.* **2012**, *118*, 536–544. [CrossRef]
32. Suliman, W.; Harsh, J.B.; Abu-Lail, N.I.; Fortuna, A.M.; Dallmeyer, I.; Garcia-Perez, M. Influence of feedstock source and pyrolysis temperature on biochar bulk and surface properties. *Biomass Bioenerg.* **2016**, *84*, 37–48. [CrossRef]
33. Brewer, C.E. Biochar Characterization and Engineering. Ph.D. Thesis, Iowa State University, Ames, IA, USA, 2012. [CrossRef]
34. Windeatt, J.H.; Ross, A.B.; Williams, P.T.; Forster, P.M.; Nahil, M.A.; Singh, S. Characteristics of biochars from crop residues: Potential for carbon sequestration and soil amendment. *J. Environ. Manag.* **2014**, *146*, 189–197. [CrossRef] [PubMed]
35. Keiluweit, M.M.; Nico, P.S.; Johnson, M.G.; Kleber, M. Dynamic molecular structure of plant biomassderived black carbon (biochar). *Environ. Sci. Technol.* **2010**, *44*, 1247–1253. [CrossRef] [PubMed]
36. Cox, J.; Downie, A.; Hickey, M.; Jenkins, A.; Lines-Kelly, R.; McClintock, A.; van Zwieten, L. *Biochar in Horticulture: Prospects for the Use of Biochar in Australian Horticulture*; HAL Report; NSW Trade and Investment: Sydney, Australia, 2012; ISBN 9781742563497.
37. Brewer, C.E.; Hu, Y.Y.; Schmidt-Rohr, K.; Loynachan, T.E.; Laird, D.A.; Brown, R.C. Extent of pyrolysis impacts on fast pyrolysis biochar properties. *J. Environ. Qual.* **2012**, *41*, 1115–1122. [CrossRef]
38. Gul, S.; Whalen, J.K.; Thomas, B.W.; Sachdeva, V.; Deng, H. Physico-chemical properties and microbial responses in biochar-amended soils: Mechanisms and future directions. *Agric. Ecosyst. Environ.* **2015**, *206*, 46–59. [CrossRef]
39. Ounas, A.; Aboulkas, A.; Harfi, K.E.; Bacaoui, A.; Yaacoubi, A. Pyrolysis of olive residue and sugar cane bagasse: Non-isothermal thermogravimetric kinetic analysis. *Bioresour. Technol.* **2011**, *102*, 11234–11238. [CrossRef]
40. Inyang, M.; Dickenson, E. The potential role of biochar in the removal of organic and microbial contaminants from potable and reuse water: Review. *Chemosphere* **2015**, *134*, 232–240. [CrossRef]
41. Greenhalf, C.E.; Nowakowski, D.J.; Harms, A.B.; Titiloye, J.O.; Bridgwater, A.V. A comparative study of straw, perennial grasses and hardwoods in terms of fast pyrolysis products. *Fuel* **2013**, *108*, 216–230. [CrossRef]
42. Qian, K.; Kumar, A.; Zhang, H.; Bellmer, D.; Huhnke, R. Recent advances in utilization of biochar. *Renew. Sustain. Energy Rev.* **2015**, *42*, 1055–1064. [CrossRef]
43. Arni, S.A. Comparison of slow and fast pyrolysis for converting biomass into fuel. *Renew. Energy* **2018**, *124*, 197–201. [CrossRef]
44. Duku, M.H.; Gu, S.; BenHagan, E. Biochar production potential in Ghana—A review. *Renew. Sust. Energ. Rev.* **2011**, *15*, 3539–3551. [CrossRef]
45. Libra, J.A.; Ro, K.S.; Kammann, C.; Funke, A.; Berge, N.D.; Neubauer, Y.; Titirici, M.-M.; Fühner, C.; Bens, O.; Kern, J.; et al. Hydrothermal carbonization of biomass residuals: A comparative review of the chemistry, processes and applications of wet and dry pyrolysis. *Biofuels* **2011**, *2*, 71–106. [CrossRef]
46. Bridgwater, A.V. Review of fast pyrolysis of biomass and product upgrading. *Biomass Bioenerg.* **2012**, *38*, 68–94. [CrossRef]
47. Liu, Z.; Quek, A.; Hoekman, S.K.; Balasubramanian, R. Production of solid biochar fuel from waste biomass by hydrothermal carbonization. *Fuel* **2013**, *103*, 943–949. [CrossRef]

48. Mumme, J.; Eckervogt, L.; Pielert, J.; Diakité, M.; Rupp, F.; Kern, J. Hydrothermal carbonization of anaerobically digested maize silage. *Bioresour. Technol.* **2011**, *102*, 9255–9560. [CrossRef]
49. Volpe, M.; Fiori, L. From olive waste to solid biofuel through hydrothermal carbonisation: The role of temperature and solid load on secondary char formation and hydrochar energy properties. *J. Anal. Appl. Pyrolysis* **2017**, *124*, 63–72. [CrossRef]
50. Riling, M.C.; Wagner, M.; Salem, M.; Antunes, P.M.; George, C.; Ramke, H.G.; Titirici, M.M.; Antonietti, M. Material derived from hydrothermal carbonization: Effects on plant growth and arbuscular mycorrhiza. *Appl. Soil Ecol.* **2010**, *45*, 238–242.
51. Cui, X.; Antonietti, M.; Yu, S.H. Structural effects of iron oxide nanoparticles and iron ions on the hydrothermal carbonization of starch and rice carbohydrates. *Small* **2006**, *2*, 756–759. [CrossRef]
52. Zheng, J.; Liu, Z.; Liu, X.; Yan, X.; Li, D.; Chu, W. Facile hydrothermal synthesis and characteristics of B-doped TiO_2 hybrid microspheres with higher photo-catalytic activity. *J. Alloys Compd.* **2011**, *509*, 3771–3776. [CrossRef]
53. Danso-Boateng, E.; Holdich, R.G.; Shama, G.; Wheatley, A.D.; Sohail, M.; Martin, S.J. Kinetics of faecal biomass hydrothermal carbonisation for hydrochar production. *Appl. Energy* **2013**, *111*, 351–357. [CrossRef]
54. Zhao, P.; Shen, Y.; Ge, S.; Yoshikawa, K. Energy recycling from sewage sludge by producing solid biofuel with hydrothermal carbonization. *Energy Convers. Manag.* **2014**, *78*, 815–821. [CrossRef]
55. Oliveira, I.; Blöhse, D.; Ramke, H.G. Hydrothermal carbonization of agricultural residues. *Bioresour. Technol.* **2013**, *142*, 138–146. [CrossRef] [PubMed]
56. Funke, A.; Ziegler, F. Hydrothermal carbonization of biomass: A summary and discussion of chemical mechanisms for process engineering. *Biofuel. Bioprod. Biorefin.* **2010**, *4*, 160–177. [CrossRef]
57. Ruiz, H.A.; Rodríguez-Jasso, R.M.; Fernandes, B.D.; Vicente, A.A.; Teixeira, J.A. Hydrothermal processing, as an alternative for upgrading agriculture residues and marine biomass according to the biorefinery concept: A review. *Renew. Sustain. Energy Rev.* **2013**, *21*, 35–51. [CrossRef]
58. Roman, S.; Nabais, J.M.V.; Laginhas, C.; Ledesma, B.; Gonzalez, J.F. Hydrothermal carbonization as an effective way of densifying the energy content of biomass. *Fuel Process. Technol.* **2012**, *103*, 78–83. [CrossRef]
59. Sabio, E.; Alvarez-Murillo, A.; Roman, S.; Ledesma, B. Conversion of tomato-peel waste into solid fuel by hydrothermal carbonization: Influence of the processing variables. *Waste Manag.* **2016**, *47*, 122–132. [CrossRef]
60. Barin, G.B.; Gimenez, I.F.; Costa, L.P.; Filho, A.G.S.; Barreto, L.S. Hollow carbon nanostructures obtained from hydrothermal carbonization of lignocellulosic biomass. *J. Mater. Sci.* **2014**, *49*, 665–672. [CrossRef]
61. Sevilla, M.; Fuertes, A.B. Chemical and structural properties of carbonaceous products obtained by hydrothermal carbonization of saccharides. *Chem. Eur. J.* **2009**, *15*, 4195–4203. [CrossRef]
62. Regmi, P.; Moscoso, J.L.G.; Kumar, S.; Cao, X.; Mao, J.; Schafran, G. Removal of copper and cadmium from aqueous solution using switchgrass biochar produced via hydrothermal carbonization process. *J. Environ. Manag.* **2012**, *109*, 61–69. [CrossRef]
63. Sun, K.; Ro, K.; Guo, M.; Novak, J.; Mashayekhi, H.; Xing, B. Sorption of bisphenol A, 17a ethinyl estradiol and phenanthrene on thermally and hydrothermally produced biochars. *Bioresour. Technol.* **2011**, *102*, 5757–5763. [CrossRef]
64. Wu, J.; Yang, J.; Huang, G.; Xu, C.; Lin, B. Hydrothermal carbonization synthesis of cassava slag biochar with excellent adsorption performance for rhodamine b. *J. Clean. Prod.* **2020**, *251*, 119717. [CrossRef]
65. Zhou, N.; Chen, H.; Xi, J.; Yao, D.; Zhou, Z.; Tian, Y.; Lu, X. Biochars with excellent Pb(II) adsorption property produced from fresh and dehydrated banana peels via hydrothermal carbonization. *Bioresour. Technol.* **2017**, *232*, 204–210. [CrossRef] [PubMed]
66. Bai, C.-X.; Shen, F.; Qi, X.-H. Preparation of porous carbon directly from hydrothermal carbonization of fructose and phloroglucinol for adsorption of tetracycline. *Chinese Chem. Lett.* **2017**, *28*, 960–962. [CrossRef]
67. Elaigwu, S.E.; Rocher, V.; Kyriakou, G.; Greenway, G.M. Removal of pb^{2+} and Cd^{2+} from aqueous solution using chars from pyrolysis and microwave-assisted hydrothermal carbonization of prosopis africana shell. *J. Ind. Eng. Chem.* **2014**, *20*, 3467–3473. [CrossRef]
68. Liu, Z.; Zhang, F.-S.; Wu, J. Characterization and application of chars produced from pinewood pyrolysis and hydrothermal treatment. *Fuel* **2010**, *89*, 510–514. [CrossRef]

69. Flora, J.F.R.; Lu, X.; Li, L.; Flora, J.R.V.; Berge, N.D. The effects of alkalinity and acidity of processwater and hydrochar washing on the adsorption of atrazine on hydrothermally produced hydrochar. *Chemosphere* **2013**, *93*, 1989–1996. [CrossRef]
70. Liang, J.; Liu, Y.; Zhang, J. Effect of solution pH on the carbon microsphere synthesized by hydrothermal carbonization. *Procedia Environ. Sci. C* **2011**, *11*, 1322–1327. [CrossRef]
71. Reza, M.T.; Rottler, E.; Herklotz, L.; Wirth, B. Hydrothermal carbonization (HTC) of wheat straw: Influence of feedwater ph prepared by acetic acid and potassium hydroxide. *Bioresour. Technol.* **2015**, *182*, 336–344. [CrossRef]
72. Skoulou, V.; Koufodimos, G.; Samaras, Z.; Zabaniotou, A. Low temperature gasification of olive kernels in a 5-kW fluidized bed reactor for H_2-rich producer gas. *Int. J. Hydrogen Energy* **2008**, *33*, 6515–6524. [CrossRef]
73. Hernández, J.J.; Lapuerta, M.; Monedero, E. Characterisation of residual char from biomass gasification: Effect of the gasifier operating conditions. *J. Clean. Prod.* **2016**, *138*, 83–93. [CrossRef]
74. García-García, A.; Gregorio, A.; Franco, C.; Pinto, F.; Boavida, D.; Gulyurtlu, I. Unconverted chars obtained during biomass gasification on a pilot-scale gasifier as a source of activated carbon production. *Bioresour. Technol.* **2003**, *88*, 27–32. [CrossRef]
75. Galhetas, M.; Mestre, A.S.; Pinto, M.L.; Gulyurtlu, I.; Lopes, H.; Carvalho, A.P. Chars from gasification of coal and pine activated with K_2CO_3: Acetaminophen and caffeine adsorption from aqueous solutions. *J. Colloid Interf. Sci.* **2014**, *433*, 94–103. [CrossRef] [PubMed]
76. Rousset, P.; Aguiar, C.; Labbé, N.; Commandré, J.-M. Enhancing the combustible properties of bamboo by torrefaction. *Bioresour. Technol.* **2011**, *102*, 8225–8231. [CrossRef] [PubMed]
77. Zhang, C.Y.; Ho, S.H.; Chen, W.H.; Fu, Y.J.; Chang, J.S.; Bi, X.T. Oxidative torrefaction of biomass nutshells: Evaluations of energy efficiency as well as biochar transportation and storage. *Appl. Energy* **2019**, *235*, 428–441. [CrossRef]
78. Li, L.; Yang, M.; Lu, Q.; Zhu, W.; Ma, H.; Dai, L. Oxygen-rich biochar from torrefaction: A versatile adsorbent for water pollution control. *Bioresour. Technol.* **2019**, *294*, 122142. [CrossRef]
79. Salapa, I.; Haralampous, P.; Giakoumakis, G.; Nazos, A.; Sidiras, D. Torrefaction of barley straw for the co-production of energy and adsorbent materials. In Proceedings of the 4th World Congress on Mechanical, Chemical, and Material Engineering (MCM'18), Madrid, Spain, 16–18 August 2018.
80. Michal, K.; Isabel, H.; Thomas, D.B.; Barbara, C.; Jadwiga, S.Z.; Patryk, O. Activated biochars reduce the exposure of polycyclic aromatic hydrocarbons in industrially contaminated soils. *Chem. Eng. J.* **2017**, *310*, 33–40.
81. Vithanage, M.; Rajapaksha, A.U.; Dou, X.; Bolan, N.S.; Yang, J.E.; Ok, Y.S. Surface complexation modeling and spectroscopic evidence of antimony adsorption on ironoxide-rich red earth soils. *J. Colloid Interf. Sci.* **2013**, *406*, 217–224. [CrossRef]
82. Liu, W.J.; Jiang, H.; Yu, H.Q. Development of biochar-based functional materials: Toward a sustainable platform carbon material. *Chem. Rev.* **2015**, *115*, 12251–12285. [CrossRef]
83. Zhang, Y.J.; Xing, Z.J.; Duan, Z.K.; Li, M.; Wang, Y. Effects of steam activation on the pore structure and surface chemistry of activated carbon derived from bamboo waste. *Appl. Surf. Sci.* **2014**, *315*, 279–286. [CrossRef]
84. Xiong, Z.; Zhang, S.; Yang, H.; Shi, T.; Chen, Y.; Chen, H. Influence of NH_3/CO_2 modification on the characteristic of biochar and the CO_2 capture. *Bioenergy Res.* **2013**, *6*, 1147–1153. [CrossRef]
85. Zhang, J.; Fan, L.; Shao, L.; He, P. The use of biochar-amended composting to improve the humifianion and degradation of sewage sludge. *Bioresour. Technol.* **2014**, *168*, 252–258. [CrossRef]
86. Peng, P.; Lang, Y.H.; Wang, X.M. Adsorption behavior and mechanism of pentachlorophenol on reed biochars: pH effect, pyrolysis temperature, hydrochloric acid treatment and isotherms. *Ecol. Eng.* **2016**, *90*, 225–233. [CrossRef]
87. Mahmoud, D.K.; Salleh, M.A.M.; Karim, W.A.W.A.; Idris, A.; Abidin, Z.Z. Batch adsorption of basic dye using acid treated kenaf fibre char: Equilibrium, kinetic and thermodynamic studies. *Chem. Eng. J.* **2012**, *181–182*, 449–457. [CrossRef]
88. Zhou, Z.; Liu, Y.; Liu, S.; Liu, H.; Zeng, G.; Tan, X.; Yang, C.; Ding, Y.; Yan, Z.; Cai, X. Sorption performance and mechanisms of arsenic(V) removal by magnetic gelatin-modified biochar. *Chem. Eng. J.* **2017**, *314*, 223–231. [CrossRef]

89. Vithanage, M.; Rajapaksha, A.U.; Zhang, M.; Thielebruhn, S.; Lee, S.S.; Ok, Y.S. Acid activated biochar increased sulfamethazine retention in soils. *Environ. Sci. Pollut. Control. Ser.* **2015**, *22*, 2175–2186. [CrossRef]
90. Jing, X.R.; Wang, Y.Y.; Liu, W.J.; Wang, Y.K.; Jiang, H. Enhanced adsorption performance of tetracycline in aqueous solutions by methanol-modified biochar. *Chem. Eng. J.* **2014**, *248*, 168–174. [CrossRef]
91. Shen, Y.; Zhang, N. Facile synthesis of porous carbons from silica-rich rice husk char for volatile organic compounds (VOCs) sorption. *Bioresour. Technol.* **2019**, *282*, 294–300. [CrossRef]
92. Cazetta, A.L.; Vargas, A.M.M.; Nogami, E.M.; Kunita, M.H.; Guilherme, M.R.; Martins, A.C.; Silva, T.L.; Moraes, J.C.G.; Almeida, V.C. NaOH-activated carbon of high surface area produced from coconut shell: Kinetics and equilibrium studies from the methylene blue adsorption. *Chem. Eng. J.* **2011**, *174*, 117–125. [CrossRef]
93. Iriarte-Velasco, U.; Ayastuy, J.; Zudaire, L.; Sierra, I. An insight into the reactions occurring during the chemical activation of bone char. *Chem. Eng. J.* **2014**, *251*, 217–227. [CrossRef]
94. Xue, Y.W.; Gao, B.; Yao, Y.; Inyang, M.; Zhang, M.; Zimmerman, A.R.; Ro, K.S. Hydrogen peroxide modification enhances the ability of biochar (hydrochar) produced from hydrothermal carbonization of peanut hull to remove aqueous heavy metals: Batch and column tests. *Chem. Eng. J.* **2012**, *200*, 673–680. [CrossRef]
95. Tan, X.; Liu, S.; Liu, Y.; Gu, Y.; Zeng, G.; Hu, X.; Wang, X.; Liu, S.; Jiang, L. Biochar as potential sustainable precursors for activated carbon production: Multiple applications in environmental protection and energy storage. *Bioresour. Technol.* **2017**, *227*, 359–372. [CrossRef]
96. Wang, H.; Gao, B.; Wang, S.; Fang, J.; Xue, Y.; Yang, K. Removal of Pb(II), Cu(II), and Cd(II) from aqueous solutions by biochar derived from $KMnO_4$ treated hickory wood. *Bioresour. Technol.* **2015**, *19*, 356–362. [CrossRef] [PubMed]
97. Thang, P.Q.; Jitae, K.; Giang, N.M.V.B.L.; Huong, P.T. Potential application of chicken manure biochar towards toxic phenol and 2, 4-dinitrophenol in wastewaters. *J. Environ. Manag.* **2019**, *251*, 109556. [CrossRef]
98. Mohammed, N.A.S.; Abu-Zurayk, R.A.; Hamadneh, I.; Al-Dujaili, A.H. Phenol adsorption on biochar prepared from the pine fruit shells: Equilibrium, kinetic and thermodynamics studies. *J. Environ. Manag.* **2018**, *226*, 377–385. [CrossRef]
99. Oh, S.-Y.; Seo, Y.-D. Factors affecting the sorption of halogenated phenols onto polymer/ biomass derived biochar: Effects of pH, hydrophobicity, and deprotonation. *J. Environ. Manag.* **2019**, *232*, 145–152. [CrossRef]
100. Qiu, Y.; Zheng, Z.; Zhou, Z.; Sheng, G.D. Effectiveness and mechanisms of dye adsorption on a strawbased biochar. *Bioresour. Technol.* **2009**, *100*, 5348–5351. [CrossRef]
101. Ferreira, C.I.A.; Calisto, V.; Otero, M.; Nadais, H.; Esteves, V.I. Comparative adsorption evaluation of biochars from paper mill sludge with commercial activated carbon for the removal of fish anaesthetics from water in recirculating aquaculture systems. *Aquac. Eng.* **2016**, *74*, 76–83. [CrossRef]
102. Jiang, S.; Huang, L.; Nguyen, T.A.H.; Ok, Y.S.; Rudolph, V.; Yang, H.; Zhang, D. Copper and zinc adsorption by softwood and hardwood biochars under elevated sulphate- induced salinity and acidic pH conditions. *Chemosphere* **2016**, *142*, 64–71. [CrossRef]
103. Jin, H.; Hanif, M.; Capareda, S.; Chang, Z.; Huang, H.; Ai, Y. Copper (II) removal potential from aqueous solution by pyrolysis biochar derived from anaerobically digested algae-dairy manure and effect of KOH activation. *J. Environ. Chem. Eng.* **2016**, *4*, 365–372. [CrossRef]
104. Ni, B.-J.; Huang, Q.-S.; Wang, C.; Ni, T.-Y.; Sun, J.; Wei, W. Competitive adsorption of heavy metals in aqueous solution onto biochar derived from anaerobically digested sludge. *Chemosphere* **2019**, *219*, 351–357. [CrossRef]
105. Park, J.; Ok, Y.S.; Kim, S.; Cho, J.; Heo, J.; Delaune, R.D.; Seo, D. Competitive adsorption of heavy metals onto sesame straw biochar in aqueous solutions. *Chemosphere* **2016**, *142*, 77–83. [CrossRef]
106. Chen, T.; Zhang, Y.; Wang, H.; Lu, W.; Zhou, Z.; Zhang, Y.; Ren, L. Influence of pyrolysis temperature on characteristics and heavy metal adsorptive performance of biochar derived from municipal sewage sludge. *Bioresour. Technol.* **2014**, *164*, 47–54. [CrossRef]
107. Zhao, M.; Dai, Y.; Zhang, M.; Feng, C.; Qin, B.; Zhang, W.; Zhao, N.; Li, Y.; Ni, Z.; Xu, Z.; et al. Mechanisms of Pb and/or Zn adsorption by different biochars: Biochar characteristics, stability, and binding energies. *Sci. Total Environ.* **2020**, *717*, 136894. [CrossRef]
108. Jingjian, P.; Jun, J.; Renkou, X. Adsorption of Cr(III) from acidic solutions by crop straw derived biochars. *J. Environ. Sci. China* **2013**, *25*, 1957–1965.

109. Park, J.; Wang, J.; Kim, S.; Cho, J.; Kang, S.; Delaune, R.; Han, K.; Seo, D. Recycling of rice straw through pyrolysis and its adsorption behaviors for cu and zn ions in aqueous solution. *Colloids Surf. A Physicochem. Eng. Asp.* **2017**, *533*, 330–337. [CrossRef]
110. Xu, X.; Cao, X.; Zhao, L.; Zhou, H.; Luo, Q. Interaction of organic and inorganic fractions of biochar with pb(II) ion: Further elucidation of mechanisms for pb(II) removal by biochar. *RSC Adv.* **2014**, *4*, 44930. [CrossRef]
111. Liu, L.; Fan, S. Removal of cadmium in aqueous solution using wheat straw biochar: Effect of minerals and mechanism. *Environ. Sci. Pollut. Res.* **2018**, *25*, 8688–8700. [CrossRef]
112. Kołodyńska, D.; Krukowska, J.; Thomas, P. Comparison of sorption and desorption studies of heavy metal ions from biochar and commercial active carbon. *Chem. Eng. J.* **2017**, *307*, 353–363. [CrossRef]
113. Fang, J.; Gao, B.; Zimmerman, A.R.; Ro, K.S.; Chen, J. Physically (CO_2) activated hydrochars from hickory and peanut hull: Preparation, characterization, and sorption of methylene blue, lead, copper, and cadmium. *RSC Adv.* **2016**, *6*, 24906–24911. [CrossRef]
114. Samsuri, A.W.; Sadegh-Zadeh, F.; Seh-Bardan, B.J. Adsorption of As(III) and As(V) by Fe coated biochars and biochars produced from empty fruit bunch and rice husk. *J. Environ. Chem. Eng.* **2013**, *1*, 981–988. [CrossRef]
115. Uchimiya, M.; Wartelle, L.H.; Klasson, K.T.; Fortier, C.A.; Lima, I.M. Influence of pyrolysis temperature on biochar property and function as a heavy metal sorbent in soil. *J. Agric. Food Chem.* **2011**, *59*, 2501–2510. [CrossRef] [PubMed]
116. Gwenzi, W.; Nyamadzawo, G. Hydrological impacts of urbanization and urban roof water harvesting in water-limited catchments: A review. *Environ. Process.* **2014**, *1*, 573–593. [CrossRef]
117. Rosales, E.; Meijide, J.; Pazos, M.; Sanroman, M.A. Challenges and recent advances in biochar as lowcost biosorbent: From batch assays to continuous-flow systems. *Bioresour. Technol.* **2017**, *246*, 176–192. [CrossRef]
118. Pignatello, J.J. *Interactions of Anthropogenic Organic Chemicals with Natural Organic Matter and Black Carbon in Environmental Particles. Biophysico-Chemical Processes of Anthropogenic Organic Compounds in Environmental Systems*; John Wiley Sons, Inc.: Hoboken, NJ, USA, 2011; pp. 1–50.
119. Ahmad, M.; Rajapaksha, A.U.; Lim, J.E.; Zhang, M.; Bolan, N.; Mohan, D.; Vithanage, M.; Lee, S.S.; Ok, Y.S. Biochar as a sorbent for contaminant management in soil and water: A review. *Chemosphere* **2014**, *99*, 19–33. [CrossRef] [PubMed]
120. Qambrani, N.A.; Rahman, M.M.; Won, S.; Shim, S.; Ra, C. Biochar properties and ecofriendly applications for climate change mitigation, waste management, and wastewater treatment: A review. *Renew. Sustain. Energy Rev.* **2017**, *79*, 255–273. [CrossRef]
121. Lu, H.; Zhang, W.; Yang, Y.; Huang, X.; Wang, S.; Qiu, R. Relative distribution of Pb^{2+} sorption mechanisms by sludge-derived biochar. *Water Res.* **2012**, *46*, 854–862. [CrossRef]
122. Zazycki, M.A.; Godinho, M.; Perondi, D.; Foletto, E.L.; Collazzo, G.C.; Dotto, G.L. New biochar from pecan nutshells as an alternative adsorbent for removing reactive red 141 from aqueous solutions. *J. Clean. Prod.* **2018**, *171*, 57–65. [CrossRef]
123. Mohamed, E.M.; Gehan, M.N.; Nabila, M.E.M.; Heba, I.B.; Sandeep, K.; Tarek, M.A.F. Kinetics, isotherm, and thermodynamic studies of the adsorption of reactive red 195 A dye from water by modified switchgrass biochar adsorbent. *J. Ind. Eng. Chem.* **2016**, *37*, 156–167.
124. Sun, P.; Hui, C.; Khan, R.A.; Du, J.; Zhang, Q.; Zhao, Y.H. Efficient removal of crystal violet using Fe_3O_4-coated biochar: The role of the Fe_3O_4 nanoparticles and modelling study their adsorption behavior. *Sci. Rep.* **2015**, *5*, 12638. [CrossRef]
125. Thines, K.R.; Abdullah, E.C.; Mubarak, N.M. Effect of process parameters for production of microporous magnetic biochar derived from agriculture waste biomass. *Microporous Mesoporous Mater.* **2017**, *253*, 29–39. [CrossRef]
126. Yakout, S.M. Physicochemical characteristics of biochar produced from rice straw at different pyrolysis temperature for soil amendment and removal of organics. *Proc. Natl. Acad. Sci. India A* **2017**, *87*, 207–214. [CrossRef]
127. Jian, X.; Zhuang, X.; Li, B.; Xu, X.; Wei, Z.; Song, Y.; Jiang, E. Comparison of characterization and adsorption of biochars produced from hydrothermal carbonization and pyrolysis. *Environ. Technol. Innov.* **2018**, *10*, 27–35. [CrossRef]
128. Huff, M.D.; Marshall, S.; Saeed, H.A.; Lee, J.W. Surface oxygenation of biochar through ozonization for dramatically enhancing cation exchange capacity. *Bioresour. Bioprocess.* **2018**, *5*, 18. [CrossRef]

129. Akl, M.A.A.; Dawy, M.B.; Serage, A.A. Efficient removal of phenol from water samples using sugarcane bagasse based activated carbon. *J. Anal. Bioanal. Tech.* **2014**, *5*, 1000189. [CrossRef]
130. Liu, Z.; Zhang, F.-S. Removal of copper (II) and phenol from aqueous solution using porous carbons derived from hydrothermal chars. *Desalination* **2011**, *267*, 101–106. [CrossRef]
131. Li, Y.; Tsend, N.; Li, T.; Liu, H.; Yang, R.; Gai, X.; Wang, H.; Shan, S. Microwave assisted hydrothermal preparation of rice straw hydrochars for adsorption of organics and heavy metals. *Bioresour. Technol.* **2019**, *273*, 136–143. [CrossRef]
132. Li, Y.; Meas, A.; Shan, S.; Yang, R.; Gai, X. Production and optimization of bamboo hydrochars for adsorption of congo red and 2-naphthol. *Bioresour. Technol.* **2016**, *207*, 379–386. [CrossRef]
133. Marfíl, A.P.; Ocampo-Pérez, R.; Collins-Martínez, V.H.; Flores-Vélez, L.M.; Gonzalez-Garcia, R.; Medellín-Castillo, N.A.; Labrada-Delgado, G.J. Synthesis and characterization of hydrochar from industrial capsicum annuum seeds and its application for the adsorptive removal of methylene blue from water. *Environ. Res.* **2020**, *184*, 109334. [CrossRef]
134. Duan, X.; Hong, W.; Srinivasakannan, C.; Wang, X. Hydrochar silicate composite sorbent via simple hydrothermal carbonization and its application to methylene blue removal. *Mater. Res. Express* **2018**, *6*, 035601. [CrossRef]
135. Nguyen, D.H.; Tran, H.N.; Chao, H.P.; Lin, C.C. Effect of nitric acid oxidation on the surface of hydrochars to sorb methylene blue: An adsorption mechanism comparison. *Adsorpt. Sci. Technol.* **2019**, *37*, 607–622. [CrossRef]
136. Kılıc, M.; Mutlu, Ç.K.Ö.Ç.; Pütün, A.E. Adsorption of heavy metal ions from aqueous solutions by bio-char, a by-product of pyrolysis. *Appl. Surf. Sci.* **2013**, *283*, 856–862. [CrossRef]
137. Wu, W.; Li, J.; Lan, T.; Müller, K.; Niazi, N.K.; Chen, X.; Xu, S.; Zheng, L.; Chu, Y.; Li, J.; et al. Unraveling sorption of lead in aqueous solutions by chemically modified biochar derived from coconut fiber: A microscopic and spectroscopic investigation. *Sci. Total Environ.* **2017**, *576*, 766–774. [CrossRef] [PubMed]
138. Shakya, A.; Agarwal, T. Removal of Cr(VI) from water using pineapple peel derived biochars: Adsorption potential and re-usability assessment. *J. Mol. Liq.* **2019**, *293*, 111497. [CrossRef]
139. Arán, D.; Antelo, J.; Fiol, S.; Mac'ıas, F. Influence of feedstock on the copper removal capacity of wastederived biochars. *Bioresour. Technol.* **2016**, *212*, 199–206. [CrossRef] [PubMed]
140. Wang, S.; Gao, B.; Zimmerman, A.R.; Li, Y.; Ma, L.; Harris, W.G.; Migliaccio, K.W. Physicochemical and sorptive properties of biochars derived from woody and herbaceous biomass. *Chemosphere* **2015**, *134*, 257–262. [CrossRef] [PubMed]
141. Bogusz, A.; Nowak, K.; Stefaniuk, M.; Dobrowolski, R.; Oleszczuk, P. Synthesis of biochar from residues after biogas production with respect to cadmium and nickel removal from wastewater. *J. Environ. Manag.* **2017**, *201*, 268–276. [CrossRef]
142. Shah, G.M.; Nasir, M.; Imran, M.; Bakhat, H.F.; Rabbani, F.; Sajjad, M.; Farooq, A.B.U.; Ahmad, S.; Song, L. Biosorption potential of natural, pyrolysed and acid-assisted pyrolysed sugarcane bagasse for the removal of lead from contaminated water. *PeerJ* **2018**, *6*, e5672. [CrossRef]
143. Abdelhafez, A.A.; Li, J. Removal of pb(II) from aqueous solution by using biochars derived from sugar cane bagasse and orange peel. *J. Taiwan. Inst. Chem. Eng.* **2016**, *61*, 367–375. [CrossRef]
144. Deng, J.; Li, X.; Wei, X.; Liu, Y.; Liang, J.; Tanga, N.; Song, B.; Chen, X.; Cheng, X. Sulfamic acid modified hydrochar derived from sawdust for removal of benzotriazole and Cu(II) from aqueous solution: Adsorption behavior and mechanism. *Bioresour. Technol.* **2019**, *290*, 121765. [CrossRef]
145. Runtti, H.; Tuomikoski, S.; Kangas, T.; Lassi, U.; Kuokkanena, T.; Rämö, J. Chemically activated carbon residue from biomass gasification as a sorbent for iron(II), copper(II) and nickel(II) ions. *J. Water Process. Eng.* **2014**, *4*, 12–24. [CrossRef]
146. Lowell, S.; Shields, J.E.; Thomas, M.A.; Thommes, M. *Characterisation of Porus Solids and Powders: Surface Area, Pore Size and Density*, 4th ed.; Springer Science & Business Media: Dordrecht, The Netherlands, 2004.
147. Zabaniotou, A.; Stavropoulos, G.; Skoulou, V. Activated carbon from olive kernels in a two-stage process: Industrial improvement. *Bioresour. Technol.* **2008**, *99*, 320–326. [CrossRef] [PubMed]
148. Mosher, K. The Impact of Pore Size on Methane and CO_2 Adsorption in Carbon. Master's Thesis, Stanford University, Stanford, CA, USA, June 2011.
149. Zhou, Z.; Shi, D.; Qiu, Y.; Sheng, G.D. Sorptive domains of pine chars as probed by benzene and nitrobenzene. *Environ. Pollut.* **2010**, *158*, 201–206. [CrossRef] [PubMed]

150. Daifullah, A.A.M.; Girgis, B.S. Removal of some substituted phenols by activated carbon obtained from agricultural waste. *Water Res.* **1998**, *32*, 1169–1177. [CrossRef]
151. Gascó, G.; Paz-Ferreiro, J.; Álvarez, M.L.; Saa, A.; Méndez, A. Biochars and hydrochars prepared by pyrolysis and hydrothermal carbonisation of pig manure. *J. Waste Manag.* **2018**, *79*, 395–403. [CrossRef] [PubMed]
152. Moreno-Castilla, C. Adsorption of organic molecules from aqueous solutions on carbon materials. *Carbon* **2004**, *42*, 83–94. [CrossRef]
153. Li, L.; Quinlivan, P.A.; Knappe, D.R.U. Effects of activated carbon surface chemistry and pore structure on the adsorption of organic contaminants from aqueous solution. *Carbon* **2002**, *40*, 2085–2100. [CrossRef]
154. Kumar, P.S.; Ramalingam, S.; Sathishkumar, K. Removal of methylene blue dye from aqueous solution by activated carbon prepared from cashew nut shell as a new low-cost adsorbent. *Korean J. Chem. Eng.* **2011**, *28*, 149–155. [CrossRef]
155. Kumar, S.; Loganathan, V.A.; Gupta, R.B.; Barnett, M.O. An assessment of U(VI) removal from groundwater using biochar produced from hydrothermal carbonization. *J. Environ. Manag.* **2011**, *92*, 2504–2512. [CrossRef]
156. Schwarzenbach, R.P.; Gschwend, P.M.; Imboden, D.M. Sorption I: General introduction and sorption processes involving organic matter. In *Environmental Organic Chemistry*; John Wiley & Sons, Inc.: Hoboken, NJ, USA, 2005; pp. 275–330.
157. Kizito, S.; Wu, S.; Kirui, W.K.; Lei, Q.L.M.; Bah, H.; Dong, R. Evaluation of slow pyrolyzed wood and rice husks biochar for adsorption of ammonium nitrogen from piggery manure anaerobic digestate slurry. *Sci. Total Environ.* **2015**, *505*, 102–112. [CrossRef]
158. Hu, X.; Zhang, X.; Ngo, H.H.; Guo, W.; Wen, H.; Li, C.; Zhang, Y.; Ma, C. Comparison study on the ammonium adsorption of the biochars derived from different kinds of fruit peel. *Sci. Total Environ.* **2020**, *707*, 135544. [CrossRef]
159. Chen, X.; Chen, G.; Chen, L.; Chen, Y.; Lehmann, J.; McBride, M.B.; Hay, A.G. Adsorption of copper and zinc by biochars produced from pyrolysis of hardwood and corn straw in aqueous solution. *Bioresour. Technol.* **2011**, *102*, 8877–8884. [CrossRef] [PubMed]
160. Tsai, W.T.; Chen, H.R. Adsorption kinetics of herbicide paraquat in aqueous solution onto a low-cost adsorbent, swine-manure-derived biochar. *Int. J. Environ. Sci. Technol.* **2013**, *10*, 1349–1356. [CrossRef]
161. Linville, J.L.; Shen, Y.; Ignacio-de Leon, P.A.; Schoene, R.P.; Urgun-Demirtas, M. In situ biogas upgrading during anaerobic digestion of food waste amended with walnut shell biochar at bench scale. *Waste Manag. Res.* **2017**, *35*, 669–679. [CrossRef] [PubMed]
162. Murray, B.C.; Galik, C.S.; Vegh, T. *Biogas in the United States: An Assessment of Market Potential in a Carbon-Constrained Future*; Nicholas Institute for Environmental Policy Solutions, Duke University: Durham, NC, USA, 2014.
163. Fagbohungbe, M.O.; Herbert, B.M.J.; Hurst, L.; Ibeto, C.N.; Li, H.; Usmani, S.Q.; Semple, K.T. The challenges of anaerobic digestion and the role of biochar in optimizing anaerobic digestion. *J. Waste Manag.* **2017**, *61*, 236–249. [CrossRef] [PubMed]
164. Luo, C.; Lu, F.; Shao, L.; He, P. Application of eco-compatible biochar in anaerobic digestion to relieve acid stress and promote the selective colonization of functional microbes. *Water Res.* **2015**, *68*, 710–718. [CrossRef] [PubMed]
165. Lü, F.; Luo, C.; Shao, L.; He, P. Biochar alleviates combined stress of ammonium and acids by firstly enriching methanosaeta and then methanosarcina. *Water Res.* **2016**, *90*, 34–43. [CrossRef]
166. Torri, C.; Fabbri, D. Biochar enables anaerobic digestion of aqueous phase from intermediate pyrolysis of biomass. *Bioresour. Technol.* **2014**, *172*, 335–341. [CrossRef]
167. Sunyoto, N.M.S.; Zhu, M.; Zhang, Z.; Zhang, D. Effect of biochar addition on hydrogen and methane production in two-phase anaerobic digestion of aqueous carbohydrates food waste. *Bioresour. Technol.* **2016**, *219*, 29–36. [CrossRef]
168. Mumme, J.; Srocke, F.; Heeg, K.; Werner, M. Use of biochars in anaerobic digestion. *Bioresour. Technol.* **2014**, *164*, 189–197. [CrossRef]
169. Cao, G.-L.; Guo, W.-Q.; Wang, A.-J.; Zhao, L.; Xu, C.-J.; Zhao, Q.-L.; Ren, N.-Q. Enhanced cellulosic hydrogen production from lime-treated cornstalk wastes using thermophilic anaerobic microflora. *Int. J. Hydrogen Energy* **2012**, *37*, 13161–13166. [CrossRef]
170. Zhang, J.; Wang, Q.; Zheng, P.; Wang, Y. Anaerobic digestion of food waste stabilized by lime mud from papermaking process. *Bioresour. Technol.* **2014**, *170*, 270–277. [CrossRef] [PubMed]

171. Yuan, J.-H.; Xu, R.-K.; Zhang, H. The forms of alkalis in the biochar produced from crop residues at different temperatures. *Bioresour. Technol.* **2011**, *102*, 3488–3497. [CrossRef] [PubMed]
172. Lü, F.; Bize, A.; Guillot, A.; Monnet, V.; Madigou, C.; Chapleur, O.; Mazéas, L.; He, P.; Bouchez, T. Metaproteomics of cellulose methanisation under thermophilic conditions reveals a surprisingly high proteolytic activity. *ISME J.* **2014**, *8*, 88–102. [CrossRef] [PubMed]
173. Zhao, Z.; Zhang, Y.; Woodard, T.L.; Nevin, K.P.; Lovley, D.R. Enhancing syntrophic metabolism in up-flow anaerobic sludge blanket reactors with conductive carbon materials. *Bioresour. Technol.* **2015**, *191*, 140–145. [CrossRef] [PubMed]
174. Enaime, G.; Baçaoui, A.; Yaacoubi, A.; Berzio, S.; Wichern, M.; Lübken, M. Packed-bed biofilm reactor for semi-continuous anaerobic digestion of olive mill wastewater: Performances and COD mass balance analysis. *Environ. Technol.* **2019**, *6*, 1–13. [CrossRef]
175. Gehring, T.; Klang, J.; Niedermayr, A.; Berzio, S.; Immenhauser, A.; Klocke, M.; Wichern, M.; Lübken, M. Determination of methanogenic pathways through carbon isotope analysis for the two-stage anaerobic digestion of high-solids substrates. *Environ. Sci. Technol.* **2015**, *49*, 4705–4714. [CrossRef]
176. Gehring, T.; Niedermayr, A.; Berzio, S.; Immenhauser, A.; Wichern, M.; Lübken, M. Determination of the fractions of syntrophically oxidized acetate in a mesophilic methanogenic reactor trough an 12C and 13C isotope-based kinetic model. *Water Res.* **2016**, *102*, 362–373. [CrossRef]
177. VandenBerg, L.; Kennedy, K.J.; Samson, R. Anaerobic downflow stationary fixed film reactor: Performance under steady-state and non-steady conditions. *Water Sci. Technol.* **1985**, *17*, 89–102. [CrossRef]
178. Zheng, H.; Li, D.; Stanislaus, M.S.; Zhang, N.; Zhu, Q.; Hu, X.; Yang, Y. Development of a bio-zeolite fixed-bed bioreactor for mitigating ammonia inhibition of anaerobic digestion with extremely high ammonium concentration livestock waste. *Chem. Eng. J.* **2015**, *280*, 106–114. [CrossRef]
179. Chauhan, A.; Ogram, A. Evaluation of support matrices for immobilization of anaerobic consortia for efficient carbon cycling in waste regeneration. *Biochem. Biophys. Res. Commun.* **2005**, *327*, 884–893. [CrossRef]
180. Bertin, L.; Lampis, S.; Todaro, D.; Scoma, A.; Vallini, G.; Marchetti, L.; Majone, M.; Fava, F. Anaerobic acidogenic digestion of olive mill wastewaters in biofilm reactors packed with ceramic filters or granular activated carbon. *Water Res.* **2010**, *44*, 4537–4549. [CrossRef] [PubMed]
181. Enaime, G.; Nettmann, E.; Berzio, S.; Baçaoui, A.; Yaacoubi, A.; Wichern, M.; Gehring, T.; Lübken, M. Performance and microbial analysis during long-term anaerobic digestion of olive mill wastewater in a packed-bed biofilm reactor. *J. Chem. Technol. Biotechnol.* **2020**, *95*, 850–861. [CrossRef]
182. Sunyoto, N.M.S.; Zhu, M.; Zhang, Z.; Zhang, D. Effect of biochar addition and initial pH on hydrogen production from the first phase of two-phase anaerobic digestion of carbohydrates food waste. *Energy Procedia* **2017**, *105*, 379–384. [CrossRef]
183. Li, Y.; McCarthy, D.T.; Deletic, A. Escherichia coli removal in copper-zeolite-integrated stormwater biofilters: Effect of vegetation, operational time, intermittent drying weather. *Ecol. Eng.* **2016**, *90*, 234–243. [CrossRef]
184. Guest, R.M.; Schang, C.; Deletic, A.; McCarthy, D.T. Zinc-sulphate-heptahydrate coated activated carbon for microbe removal from stormwater. *Water Sci. Technol.* **2012**, *66*, 1582–1589. [CrossRef]
185. Chandrasena, G.I.; Deletic, A.; Ellerton, J.; McCarthy, D.T. Evaluating escherichia coli removal performance in stormwater biofilters: A laboratory-scale study. *Water Sci. Technol.* **2012**, *66*, 1132–1138. [CrossRef]
186. Kaetzl, K.; Lübken, M.; Uzuna, G.; Gehring, T.; Nettmann, E.; Stenchly, K.; Wichern, M. On-farm wastewater treatment using biochar from local agroresidues reduces pathogens from irrigation water for safer food production in developing countries. *Sci. Total Environ.* **2019**, *682*, 601–610. [CrossRef]
187. Chen, G.; Walker, S.L. Fecal indicator bacteria transport and deposition in saturated and unsaturated porous media. *Environ. Sci. Technol.* **2012**, *46*, 8782–8790. [CrossRef]
188. Stevik, T.K.; Aa, K.; Ausland, G.; Hanssen, J.F. Retention and removal of pathogenic bacteria in wastewater percolating through porous media: A review. *Water Res.* **2004**, *38*, 1355–1367. [CrossRef]
189. Werner, S.; Katzl, K.; Wichern, M.; Buerkert, A.; Steiner, C.; Marschner, B. Agronomic benefits of biochar as a soil amendment after its use as waste water filtration medium. *Environ. Pollut.* **2018**, *233*, 561–568. [CrossRef]
190. Dalahmeh, S.; Ahrens, L.; Gros, M.; Wiberg, K.; Pell, M. Potential of biochar filters for onsite sewage treatment: Adsorption and biological degradation of pharmaceuticals in laboratory filters with active, inactive and no biofilm. *Sci. Total Environ.* **2018**, *612*, 192–201. [CrossRef] [PubMed]

191. Perez-Mercado, L.F.; Lalander, C.; Berger, C.; Dalahmeh, S.S. Potential of biochar filters for onsite wastewater treatment: Effects of biochar type, physical properties and operating conditions. *Water* **2018**, *10*, 1835. [CrossRef]
192. Lau, A.Y.T.; Tsang, D.C.W.; Graham, N.; Ok, Y.; Yang, X.; Li, X. Surface-modified biochar in a bioretention system for Escherichia coli removal from stormwater. *Chemosphere* **2017**, *169*, 89–98. [CrossRef] [PubMed]
193. Mohanty, S.K.; Boehm, A.B. Escherichia coli removal in biochar-augmented biofilter: Effect of infiltration rate, initial bacterial concentration, biochar particle size, and presence of compost. *Environ. Sci. Technol.* **2014**, *48*, 11535–11542. [CrossRef] [PubMed]
194. Moussavi, G.; Khosravi, R. Preparation and characterization of a biochar from pistachio hull biomass and its catalytic potential for ozonation of water recalcitrant contaminants. *Bioresour. Technol.* **2012**, *119*, 66–71. [CrossRef] [PubMed]
195. Xu, T.; Zhu, R.; Liu, J.; Zhou, Q.; Zhu, J.; Liang, X.; Xi, Y.; He, H. Fullerol modification ferrihydrite for the degradation of acid red 18 under simulated sunlight irradiation. *J. Mol. Catal. A Chem.* **2016**, *424*, 393–401. [CrossRef]
196. Qin, Y.; Li, G.; Gao, Y.; Zhang, L.; Ok, Y.S.; An, T. Persistent free radicals in carbon-based materials on transformation of refractory organic contaminants (rocs) in water: A critical review. *Water Res.* **2018**, *137*, 130–143. [CrossRef]
197. Yang, S.; Xiao, T.; Zhang, J.; Chen, Y.; Li, L. Activated carbon fiber as heterogeneous catalyst of peroxymonosulfate activation for efficient degradation of acid orange 7 in aqueous solution. *Sep. Purif. Technol.* **2015**, *143*, 19–26. [CrossRef]
198. Fang, G.; Zhu, C.; Dionysiou, D.D.; Gao, J.; Zhou, D. Mechanism of hydroxyl radical generation from biochar suspensions: Implications to diethyl phthalate degradation. *Bioresour. Technol.* **2015**, *176*, 210–217. [CrossRef]
199. Qin, Y.; Zhang, L.; An, T. Hydrothermal carbon-mediated fenton-like reaction mechanism in the degradation of alachlor: Direct electron transfer from hydrothermal carbon to Fe(III). *ACS Appl. Mater. Interfaces* **2017**, *9*, 17115–17124. [CrossRef]
200. Izghri, Z.; Enaime, G.; Louarrat, M.; Gaini, L.E.; Baçaoui, A.; Yaacoubi, A. Novel catalyst from two-phase olive mill wastes using hydrothermal carbonisation for the removal of methylene blue by heterogeneous fenton-like oxidation. *Int. J. Environ. Anal. Chem.* **2019**. [CrossRef]
201. Varjani, S.; Joshi, R.; Srivastava, V.K.; Ngo, H.H.; Guo, W. Treatment of wastewater from petroleum industry: Current practices and perspectives. *Environ. Sci. Pollut. Res.* **2019**. [CrossRef] [PubMed]
202. Wiedemeier, D.B.; Abiven, S.; Hockaday, W.C.; Keiluweit, M.; Kleber, M.; Masiello, C.A.; McBeath, A.V.; Nico, P.S.; Pyle, L.A.; Schneider, M.P.W.; et al. Aromaticity and degree of aromatic condensation of char. *Org. Geochem.* **2015**, *78*, 135–143. [CrossRef]
203. Huang, M.; Li, Z.; Luo, N.; Yang, R.Y.; Wen, J.; Huang, B.; Zeng, G. Application potential of biochar in environment: Insight from degradation of biocharderived dom and complexation of dom with heavy metals. *Sci. Total Environ.* **2019**, *646*, 220–228. [CrossRef] [PubMed]
204. Li, X.; Luo, J.W.; Deng, H.; Huang, P.; Ge, C.J.; Yu, H.M.; Xu, W. Effect of cassava waste biochar on sorption and release behaviour of atrazine in soil. *Sci. Total Environ.* **2018**, *644*, 1617–1624. [CrossRef]